9-4-2007

Extracellular Stimuli Specifically Regulate Localized Levels of Individual Neuronal mRNAs

Dianna E. Willis
Alfred I. duPont Hospital for Children

Erna A. van Niekerk
University of Delaware

Yukio Sasaki
Emory University

Mariano Mesngon
University of South Carolina - Columbia

Tanuja T. Merianda
Alfred I. duPont Hospital for Children

See next page for additional authors

Publication Info

The Journal of Cell Biology, Volume 178, Issue 6, 2007, pages 965-980.

Originally published in the Journal of Cell Biology by the Rockefeller University Press.

Published September 4, 2007

Extracellular stimuli specifically regulate localized levels of individual neuronal mRNAs

Dianna E. Willis,[1] Erna A. van Niekerk,[2] Yukio Sasaki,[3] Mariano Mesngon,[4] Tanuja T. Merianda,[1] Gervan G. Williams,[1] Marvin Kendall,[1] Deanna S. Smith,[4] Gary J. Bassell,[3] and Jeffery L. Twiss[1,2]

[1]Nemours Biomedical Research, Alfred I. duPont Hospital for Children, Wilmington, DE 19803
[2]Department of Biological Sciences, University of Delaware, Newark, DE 19716
[3]Department of Cell Biology, Emory University, Atlanta, GA 30322
[4]Department of Biology, University of South Carolina, Columbia, SC 29208

Subcellular regulation of protein synthesis requires the correct localization of messenger RNAs (mRNAs) within the cell. In this study, we investigate whether the axonal localization of neuronal mRNAs is regulated by extracellular stimuli. By profiling axonal levels of 50 mRNAs detected in regenerating adult sensory axons, we show that neurotrophins can increase and decrease levels of axonal mRNAs. Neurotrophins (nerve growth factor, brain-derived neurotrophic factor, and neurotrophin-3) regulate axonal mRNA levels and use distinct downstream signals to localize individual mRNAs. However, myelin-associated glycoprotein and semaphorin 3A regulate axonal levels of different mRNAs and elicit the opposite effect on axonal mRNA levels from those observed with neurotrophins. The axonal mRNAs accumulate at or are depleted from points of ligand stimulation along the axons. The translation product of a chimeric green fluorescent protein–β-actin mRNA showed similar accumulation or depletion adjacent to stimuli that increase or decrease axonal levels of endogenous β-actin mRNA. Thus, extracellular ligands can regulate protein generation within subcellular regions by specifically altering the localized levels of particular mRNAs.

Introduction

Subcellular localization of mRNAs can locally control the protein composition of distinct regions within the cell. Neurons provide an ideal system for understanding how subcellular mRNA localization is regulated. The widely separated cytoplasmic extents of neuronal dendrites, axons, and cell body allow one to ask how local extracellular stimuli may alter populations of localized mRNAs and ultimately modulate the local protein composition of that subcellular domain. Much recent effort has focused on how neuronal RNA trafficking and localized translation are regulated (Tiedge, 2005; Bassell and Twiss, 2006; Martin and Zukin, 2006). Transport of mRNAs and translational machinery into axons along with subsequent local protein synthesis is needed to initiate growth responses and for growing neurons to respond to environmental stimuli (Campbell and Holt, 2001, 2003; Ming et al., 2002; Brunet et al., 2005; Piper et al., 2005, 2006; Verma et al., 2005; Wu et al., 2005; Leung et al., 2006; Yao et al., 2006).

Despite increasing knowledge of stimuli that can trigger axonal protein synthesis, knowledge of the specificity of these autonomous responses has been quite limited (Piper and Holt, 2004). Injury of peripheral axons triggers localized translation of importin β and vimentin mRNAs, and these nascent protein products generate a retrograde signaling complex (Hanz et al., 2003; Perlson et al., 2005). In cultures of developing neurons, the guidance cue semaphorin 3A (Sema3A) activates the localized translation of RhoA mRNA (Wu et al., 2005), and neurotrophins increase the localized synthesis of axonal β-actin (Zhang et al., 1999). A study aimed at determining the scope of locally synthesized proteins argues that axons have the potential to synthesize many different proteins (Willis et al., 2005), raising the questions of if and how the expression of these proteins may be regulated in the axonal compartment.

In addition to translational control, regulating the delivery of mRNAs to subcellular regions can modulate localized protein synthesis by altering which mRNAs are locally available for translation. Evidence for this is seen in cultures of developing cortical neurons in which bath application of neurotrophins can increase the delivery of β-actin mRNA to the axonal growth cone

Correspondence to Jeffery L. Twiss: twiss@medsci.udel.edu

Abbreviations used in this paper: AV, adenovirus; BDNF, brain-derived neurotrophic factor; db-cAMP, dibutyral cAMP; DRB, 5,6-dichlorobenzimidazole riboside; DRG, dorsal root ganglion; eGFP, enhanced GFP; EHNA, erythro-9-(2-hydroxy-3-nonyl)adenine hydrochloride; GAP-43, 43-kD growth-associated protein; MAG, myelin-associated glycoprotein; NT3, neurotrophin-3; PI3K, phosphatidyl inositol-3 kinase; qPCR, quantitative PCR; Sema3A, semaphorin 3A; UTR, untranslated region.

The online version of this article contains supplemental material.

Supplemental Material can be found at:
http://jcb.rupress.org/content/suppl/2007/09/04/jcb.200703209.DC1.html

The Journal of Cell Biology, Vol. 178, No. 6, September 10, 2007 965–980
http://www.jcb.org/cgi/doi/10.1083/jcb.200703209

Published September 4, 2007

(Zhang et al., 1999). In the present study, we show that the levels of individual axonal mRNAs are differentially regulated by the local stimulation of axons with growth-promoting and growth-inhibiting stimuli. Quantitative analyses of axonal mRNAs showed that nerve growth factor (NGF), brain-derived neurotrophic factor (BDNF), neurotrophin-3 (NT3), myelin-associated glycoprotein (MAG), and Sema3A can specifically increase or decrease levels of individual transcripts. These alterations in axonal mRNA levels were accompanied by opposite changes in the cell body mRNA levels, suggesting that ligand-dependent alterations in anterograde transport rates exist. With in situ hybridization and heterologous expression of a chimeric mRNA containing the rat β-actin mRNA localization element, the alterations in axonal mRNA levels seen by quantitative analyses correspond to the relative enrichment or depletion of individual mRNAs from axonal regions directly adjacent to ligand sources. These findings argue that diverse extracellular signals bidirectionally regulate the transport of numerous mRNAs within axons to influence local protein synthesis.

Results

Scope of proteins locally synthesized in the rat sensory axons

We previously used a proteomics approach to identify locally synthesized proteins from cultures of adult rat dorsal root ganglion (DRG) neurons (Willis et al., 2005). This approach was limited to the most abundant axonally synthesized proteins. Because we were able to view only a fraction of the axonal mRNAs using this method, we reasoned that a more global assessment of axonal mRNA content would be needed to test for the specific regulation of axonal mRNA localization. For this, axonal RNA was isolated from dissociated cultures of DRG neurons after 20–22 h in vitro as previously described (Zheng et al., 2001). The L4-5 DRGs were conditioned by in vivo sciatic nerve crush 7 d before culture. These injury-conditioned sensory neurons show rapid transcription-independent, translation-dependent process outgrowth over 24 h in culture (Smith and Skene, 1997; Twiss et al., 2000). The purity of axonal preparations was verified by the absence of γ-actin and microtubule-associated protein 2 mRNAs (Fig. S1, available at http://www.jcb.org/cgi/content/full/jcb.200703209/DC1; Zheng et al., 2001; Willis et al., 2005). Amplified cDNAs prepared from axonal RNAs were used to hybridize to Atlas cDNA arrays containing ∼4,000 rat cDNAs. Localized mRNAs detected from hybridizations of four separate axonal preparations are summarized in Table S1. According to these data, the injury-conditioned DRG axons have the capacity to synthesize >200 different proteins, including transmembrane proteins (e.g., Kv3.1a and HCN4) and components of the translational machinery (e.g., ribosomal proteins) that were not detected in our previous proteomics screen (Willis et al., 2005).

Axonal mRNA levels can be positively and negatively regulated by peripheral stimulation with chemotropic agents

Guidance cues that invoke axon turning or collapse have been shown to regulate axonal protein synthesis (Campbell and Holt, 2001, 2003; Ming et al., 2002; Piper et al., 2005). To determine whether axonal mRNA localization is specifically regulated in the DRG neurons, we asked whether the local application of growth-promoting or growth-inhibiting stimuli to DRG axons can alter the localization of individual mRNAs. A panel of 50 axonal mRNAs from the aforementioned array data and a previous proteomics study (Willis et al., 2005), which broadly represents axonal mRNAs encoding different protein types, was used for these analyses. Neurotrophins were chosen for the growth-promoting ligands because their TrkA, TrkB, and TrkC receptors are expressed by all of the DRG neurons (Snider, 1994). Sema3A and MAG were used as growth-inhibitory stimuli because these ligands induce axonal retraction or repulsion in rat DRG neurons (Shen et al., 1998; Li et al., 2004). The axonal compartment was exposed to ligands immobilized on microparticles for 4 h in the presence of the RNA polymerase II inhibitor 5,6-dichlorobenzimidazole riboside (DRB). Microparticles with immobilized BSA, AP, or human IgG Fc domain were used as controls for the neurotrophin, Sema3A, and MAG, respectively. Axonal mRNA levels for each of the 50 transcripts were determined using axonal RNA isolates for reverse transcription followed by quantitative PCR (qPCR). The qPCR results are detailed in Table I. These data show both ligand and transcript specificity for the regulation of axonal mRNA levels.

Fig. 1 summarizes changes in axonal levels for a few mRNAs to illustrate the specificity of these ligand-dependent responses. Note that each stimulus can increase or decrease axonal levels of an individual mRNA. For the neurotrophins, NGF and BDNF showed an overall similar regulation of axonal mRNA levels except for 43-kD growth-associated protein (GAP-43) mRNA, which was uniquely affected by NGF (Fig. 1 A). NT3 modulation of axonal mRNA levels appeared distinct from NGF and BDNF. For example, axonal levels of the mRNA encoding the Kv3.1a potassium channel was decreased by NGF and BDNF, but NT3 increased axonal levels of Kv3.1a mRNA (Fig. 1 A). Similar to the neurotrophins, MAG and Sema3A increased and decreased the localization of individual axonal mRNAs (Fig. 1 B). With the exception of vimentin mRNA, MAG and Sema3A altered axonal mRNA levels distinctly from the neurotrophins (Fig. 1 B and Table I). For example, Sema3A and MAG decreased axonal β-actin mRNA levels, whereas the neurotrophins consistently increased axonal β-actin mRNA levels. Several transcripts that were not responsive to the neurotrophins showed altered axonal levels with MAG and/or Sema3A (Table I). Interestingly, many of the mRNAs tested showed no significant change ($P > 0.01$) in response to the 4-h ligand stimulation (Table I). This result, combined with the differences in axonal mRNA levels seen among the individual neurotrophins, indicates that the regulation of mRNA localization is highly specific at the level of individual transcripts and for ligands that activate similar intracellular signaling pathways.

Ligand-induced changes in axonal mRNAs change cell body mRNA content

Over the 4-h period used to stimulate the aforementioned axons, DRB decreased new RNA synthesis >90% based on the incorporation of α-[^{32}P]UTP into RNA isolated from cultures of

Published September 4, 2007

Table I. **Modulation of axonal mRNA levels in response to growth-promoting and growth-inhibiting stimuli**

mRNA	NGF	BDNF	NT3	MAG	Sema3A
αB crystallin	1.22 ± 0.10	1.17 ± 0.08	1.20 ± 0.16	**4.59 ± 0.24**	5.03 ± 0.13
Aldolase C	1.04 ± 0.07	−1.09 ± 0.04	**−1.75 ± 0.14**	−1.30 ± 0.25	−1.52 ± 0.21
Amphoterin	1.03 ± 0.19	1.04 ± 0.14	1.05 ± 0.18	−1.03 ± 0.16	−1.08 ± 0.15
ATP synthase	1.31 ± 0.07	1.06 ± 0.09	**−1.92 ± 0.14**	1.06 ± 0.09	1.21 ± 0.22
β-actin	**4.14 ± 0.48**	**4.41 ± 0.38**	**2.17 ± 0.13**	**−1.30 ± 0.16**	**−1.38 ± 0.19**
CACNA1	**−1.45 ± 0.11**	**−1.56 ± 0.12**	−1.19 ± 0.14	1.12 ± 0.09	1.28 ± 0.21
Calmodulin (RCM3)	1.13 ± 0.18	1.05 ± 0.25	−1.00 ± 0.16	1.10 ± 0.18	1.08 ± 0.20
Calreticulin	1.06 ± 0.10	1.21 ± 0.40	**2.22 ± 0.06**	**2.73 ± 0.15**	**4.20 ± 0.09**
Cathepsin B	−1.04 ± 0.12	−1.06 ± 0.15	1.01 ± 0.11	1.04 ± 0.13	1.06 ± 0.17
Cofilin	1.13 ± 0.05	1.04 ± 0.09	1.19 ± 0.06	−1.06 ± 0.09	−1.03 ± 0.08
CsA	1.15 ± 0.06	−1.07 ± 0.19	**−1.54 ± 0.06**	1.13 ± 0.12	−1.31 ± 0.07
Cyclophilin A	1.07 ± 0.16	1.04 ± 0.20	1.06 ± 0.17	−1.03 ± 0.16	−1.18 ± 0.15
Cystatin C	1.13 ± 0.12	1.02 ± 0.14	−1.04 ± 0.15	1.01 ± 0.20	1.01 ± 0.16
Ddah2	−1.03 ± 0.13	−1.07 ± 0.15	**−1.52 ± 0.16**	**1.43 ± 0.11**	1.13 ± 0.02
Enolase	**1.32 ± 0.08**	**1.35 ± 0.14**	−1.05 ± 0.09	1.19 ± 0.12	**−1.58 ± 0.19**
ERp29	−1.01 ± 0.08	1.03 ± 0.07	1.17 ± 0.09	1.18 ± 0.09	−1.08 ± 0.09
GAP43	**2.25 ± 0.06**	1.13 ± 0.13	−1.01 ± 0.05	−1.09 ± 0.08	−1.13 ± 0.08
GAPDH	1.07 ± 0.09	1.03 ± 0.04	−1.03 ± 0.13	−1.01 ± 0.19	−1.05 ± 0.12
grp75	−1.15 ± 0.07	−1.05 ± 0.07	1.24 ± 0.20	1.09 ± 0.16	1.14 ± 0.08
grp78/BiP	−1.03 ± 0.07	1.05 ± 0.10	1.23 ± 0.08	**1.67 ± 0.15**	**1.47 ± 0.22**
γ-Synuclein	−1.03 ± 0.07	1.02 ± 0.13	**−1.56 ± 0.05**	1.01 ± 0.15	−1.01 ± 0.06
γ-Tropomyosin 3	1.03 ± 0.07	1.03 ± 0.07	**−1.47 ± 0.06**	1.13 ± 0.10	**−1.69 ± 0.05**
HCN4	**−1.40 ± 0.17**	**−1.35 ± 0.09**	1.17 ± 0.21	1.21 ± 0.16	**2.07 ± 0.21**
hnRNPH′	1.02 ± 0.06	1.03 ± 0.10	−1.03 ± 0.08	1.23 ± 0.15	−1.13 ± 0.13
HSP27	1.08 ± 0.21	−1.03 ± 0.16	**−1.56 ± 0.08**	**−1.44 ± 0.14**	1.05 ± 0.09
HSP60	−1.13 ± 0.07	−1.13 ± 0.09	**2.36 ± 0.23**	**1.46 ± 0.13**	**2.45 ± 0.21**
HSP70	1.01 ± 0.06	−1.09 ± 0.05	**−2.27 ± 0.13**	−1.10 ± 0.16	**1.38 ± 0.17**
HSP90	−1.03 ± 0.07	1.03 ± 0.08	**−2.08 ± 0.11**	**2.53 ± 0.28**	**3.32 ± 0.14**
Importin β1	1.06 ± 0.11	1.03 ± 0.05	1.09 ± 0.15	1.06 ± 0.09	1.05 ± 0.07
Kv3.1a	**−1.79 ± 0.13**	**−1.89 ± 0.12**	**2.14 ± 0.10**	−1.04 ± 0.14	−1.03 ± 0.20
Lipocortin 2	1.06 ± 0.07	1.04 ± 0.09	1.01 ± 0.07	1.04 ± 0.08	1.09 ± 0.09
Neuritin	1.07 ± 0.11	1.06 ± 0.16	1.00 ± 0.12	1.13 ± 0.13	1.08 ± 0.09
NMP35	−1.04 ± 0.06	−1.04 ± 0.17	1.05 ± 0.14	1.10 ± 0.17	1.13 ± 0.11
PEBP	1.09 ± 0.08	−1.03 ± 0.11	**−1.45 ± 0.11**	1.14 ± 0.15	**1.52 ± 0.16**
Peripherin	**2.85 ± 0.20**	**2.85 ± 0.13**	**−1.32 ± 0.03**	1.09 ± 0.19	1.11 ± 0.11
Pgk1	1.03 ± 0.19	1.13 ± 0.16	−1.13 ± 0.21	**3.92 ± 0.13**	−1.10 ± 0.06
Prdx1	−1.03 ± 0.10	1.28 ± 0.04	−1.10 ± 0.16	**1.48 ± 0.17**	**1.36 ± 0.08**
Prdx6	1.08 ± 0.26	1.03 ± 0.21	−1.23 ± 0.05	1.29 ± 0.11	1.14 ± 0.09
RP-L11	−1.13 ± 0.11	−1.09 ± 0.12	−1.04 ± 0.15	1.10 ± 0.13	1.15 ± 0.16
RP-L22	**3.10 ± 0.07**	**2.85 ± 0.08**	1.26 ± 0.11	−1.13 ± 0.21	**−1.98 ± 0.20**
RP-L24	**2.66 ± 0.07**	**3.01 ± 0.07**	1.16 ± 0.19	−1.10 ± 0.11	−1.05 ± 0.11
RP-L37	−1.08 ± 0.13	−1.13 ± 0.17	−1.09 ± 0.19	−1.08 ± 0.19	−1.13 ± 0.18
RP-S17	**2.50 ± 0.10**	**2.60 ± 0.10**	1.09 ± 0.07	−1.14 ± 0.09	−1.12 ± 0.12
RP-S23	−1.13 ± 0.09	−1.17 ± 0.08	−1.15 ± 0.10	1.05 ± 0.10	−1.01 ± 0.09
RVDAC3	−1.03 ± 0.08	−1.04 ± 0.10	**−1.61 ± 0.17**	**1.38 ± 0.15**	−1.01 ± 0.08
SOD1	1.13 ± 0.10	1.31 ± 0.16	−1.01 ± 0.08	**1.56 ± 0.12**	**1.58 ± 0.16**
Sp22 (DJ-1)	1.12 ± 0.16	1.01 ± 0.14	**2.28 ± 0.15**	1.03 ± 0.16	**2.19 ± 0.05**
Tα1 tubulin	1.09 ± 0.08	1.15 ± 0.07	−1.09 ± 0.06	**1.44 ± 0.09**	1.20 ± 0.11
Thymosin β-4	**1.95 ± 0.06**	**1.87 ± 0.07**	**−1.64 ± 0.11**	1.01 ± 0.11	**−1.82 ± 0.14**
UchL1	1.08 ± 0.12	1.03 ± 0.15	1.07 ± 0.12	1.09 ± 0.07	1.11 ± 0.19
Vimentin	**3.56 ± 0.01**	**3.94 ± 0.21**	1.01 ± 0.07	**5.28 ± 0.16**	**4.72 ± 0.09**

qPCR data for the axonal mRNAs tested for axonal level modulation by NGF, BDNF, NT3, MAG, and Sema3A are tabulated. Axonal levels of the mRNAs are compared with axons treated with controls (BSA for NGF, BDNF, and NT-3; IgG-Fc for MAG; and AP for Sema3A) and are displayed ± SD from three replicates. Values in bold indicate differences that were statistically significant based on $P < 0.01$ by the student Newman-Keul test. The other values are not statistically significant ($P \geq 0.01$).

Published September 4, 2007

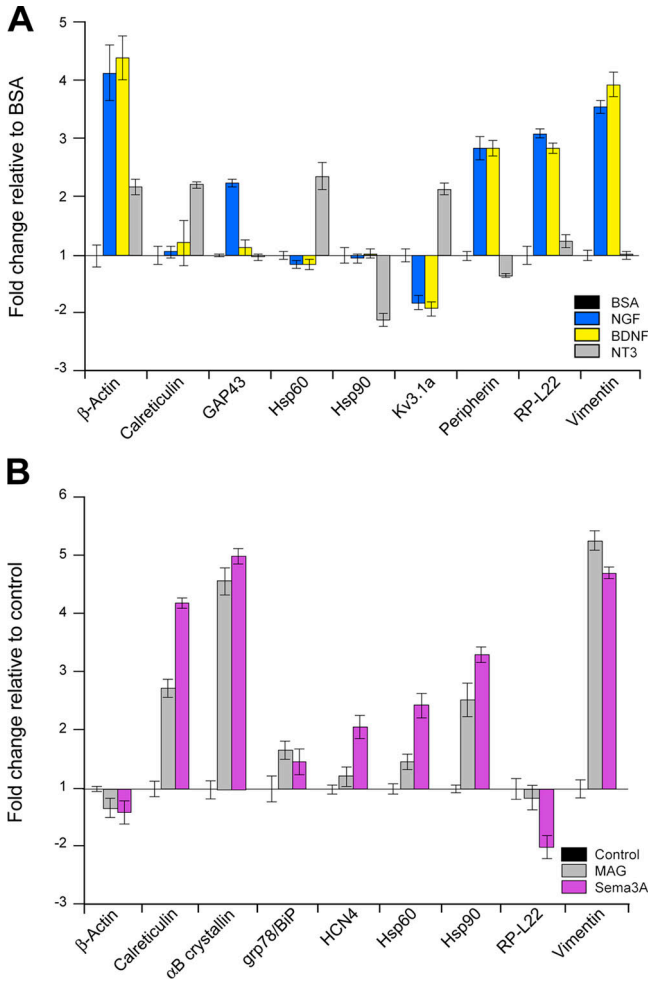

Figure 1. **Axonal stimulation with growth-promoting and growth-inhibiting stimuli alters axonal mRNA localization.** (A and B) The changes in axonal levels of representative mRNAs in response to NGF, BDNF, and NT-3 (A) or MAG-Fc and Sema3A-AP (B) from Table I are graphically illustrated. Positive values indicate an increase in axonal mRNA content, and negative values indicate a decrease in axonal mRNA content detected by qPCR. The axonal mRNA values for neurotrophins are expressed relative to axons treated with BSA. Values for MAG are expressed relative to human IgG Fc, and those for Sema3A are expressed relative to AP (there were no statistically significant differences between the Fc and AP controls; not depicted). Error bars represent the SD of three replicate experiments with each sample measured in quadruplicate. Significance was calculated based on $P \leq 0.01$ by a student Newman-Keul test compared with the control. Note that the neurotrophins, MAG, and Sema3A selectively increase or decrease the transport of individual mRNAs. No statistically significant changes were seen in axonal levels of αB crystallin, grp78/BiP, or HCN4 mRNAs with NGF, BDNF, or NT3 treatments. No statistically significant changes were seen in axonal levels of GAP43, Kv3.1a, or peripherin mRNAs with MAG or Sema3A treatments.

injury-conditioned DRGs (Fig. S2 A, available at http://www.jcb.org/cgi/content/full/jcb.200703209/DC1). Although we cannot exclude the possibility that alterations in axonal mRNA stability contributed to the changes in axonal mRNA levels, these metabolic labeling experiments suggest that chemotropic agents can alter the localization of existing mRNA populations. If this is the case, any transport-dependent changes in axonal mRNA levels should be accompanied by an opposite change in the levels of that transcript in the cell body. Although our previous analysis of cytoskeletal mRNAs did not show depletion of cell body levels

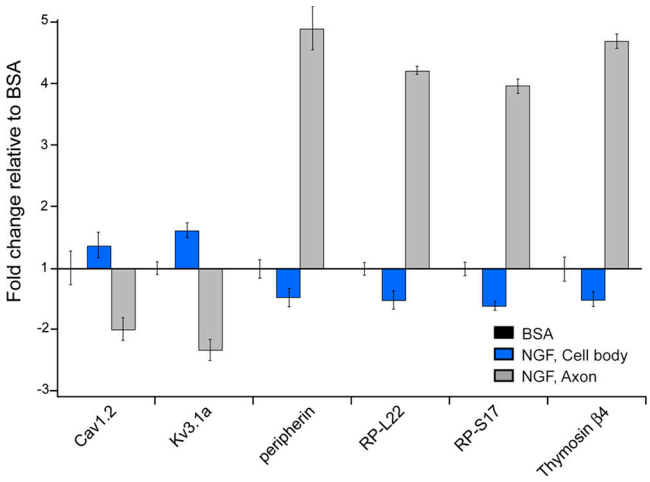

Figure 2. **Alterations in axonal mRNA levels inversely affect cell body mRNA content.** To determine whether altered transport from the cell body underlies the neurotrophin-mediated changes in axonal transcript levels, the axonal compartment of 16-h injury-conditioned DRG cultures was treated with NGF microparticles for 12 h. Duplicate cultures were treated, with one set of tissue culture inserts processed to isolate the axonal compartment RNA and the other set used to isolate the cell body compartment RNA. Levels of the indicated mRNAs were analyzed by qPCR as in Fig. 1. For each NGF-dependent change in levels of the axonal mRNA, an opposite change in the levels of that transcript was seen in the cell body RNA sample. Error bars represent the SD of three replicate experiments with each sample measured in quadruplicate.

after NGF-induced increases in mRNA levels in the axons, the high expression of cytoskeletal mRNAs in the DRG cultures could complicate the detection of cell body depletion during this and previous short-term experiments (Willis et al., 2005). To more rigorously test for ligand-dependent alterations in axonal mRNA content, we extended treatment duration from 4 to 12 h and evaluated axonal levels of a subset of mRNAs that showed increased or decreased axonal levels with NGF (Fig. 2). qPCR analyses of cell body and axonal RNA content showed that the decrease in axonal levels of $Ca_v1.2$ and Kv3.1a mRNAs seen after NGF exposure resulted in a statistically significant increase ($P \leq 0.01$) in the cell body content of these mRNAs. In contrast, increased axonal levels of peripherin, RP-L22, RP-S17, and thymosin β4 mRNAs resulted in decreased cell body mRNA content (Fig. 2). These data suggest that the sensory neurons draw on a pool of preexisting mRNAs in the cell body to alter the delivery of individual mRNAs into the axons in response to ligand stimulation. In addition, these data indicate that extracellular signals can lead to a new steady state in the distribution of specific mRNAs between the cell body and axon that is likely independent of transcription.

RNAs are transported on microfilaments in fibroblasts, whereas most other cellular systems, including neurons, have been shown to use microtubules for long-range transport of mRNAs (Sundell and Singer, 1990; Carson et al., 1997; Brumwell et al., 2002; Oleynikov and Singer, 2003; Shan et al., 2003; Chang et al., 2006). To determine whether the neurotrophin-dependent changes in axonal mRNA levels in Fig. 1 A require intact cytoskeleton, dissociated cultures were pretreated with cytochalasin D or colchicine to disrupt microfilaments or microtubules, respectively. For this analysis, we examined a subset of the transcripts

Published September 4, 2007

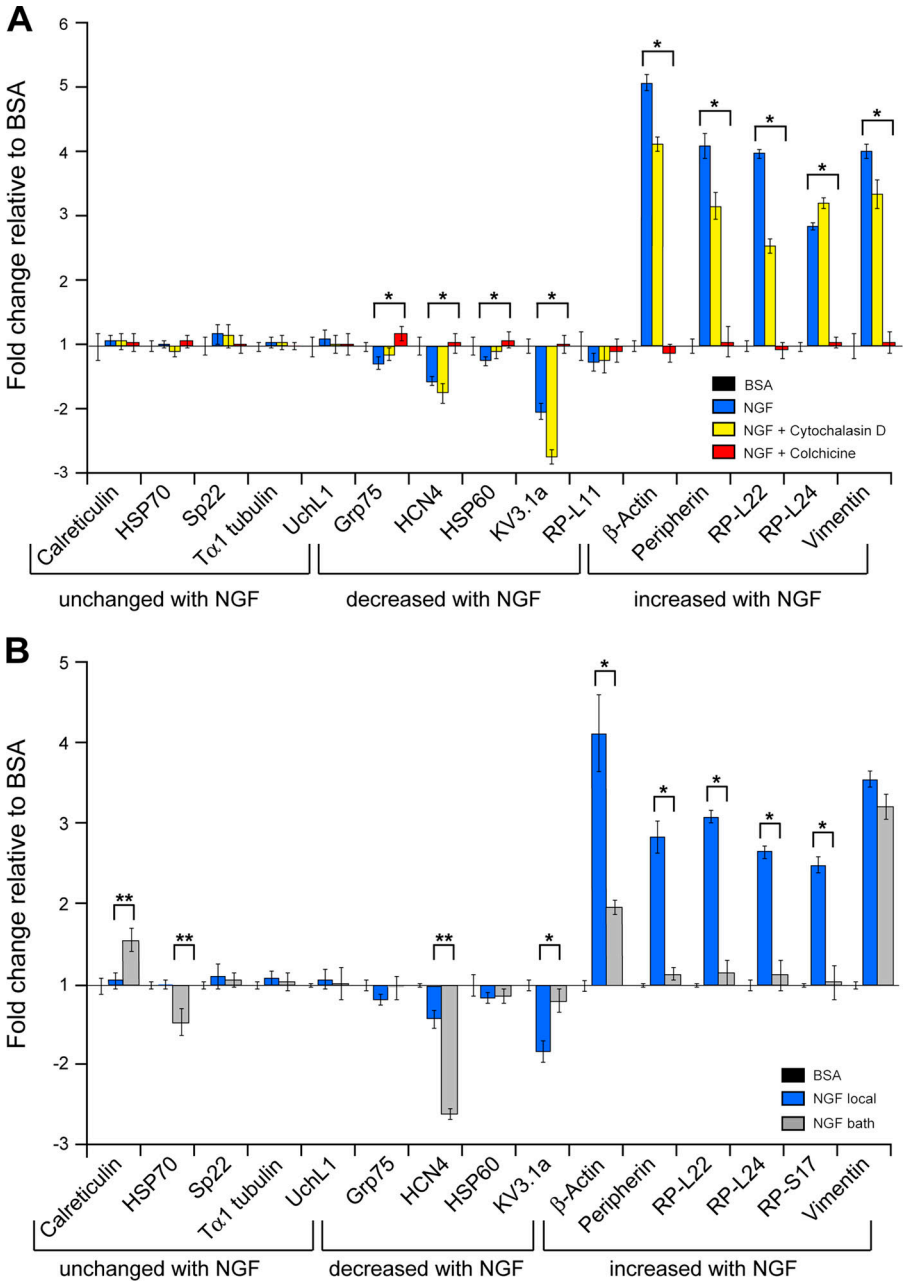

Figure 3. **Axonal stimulation of mRNA localization is microtubule based.** (A) To determine how mRNAs are transported into the axonal compartment, injury-conditioned DRG cultures were treated with cytochalasin D or colchicine for 30 min followed by exposure of the axonal compartment to NGF microparticles for 4 h as indicated. Levels of the axonal mRNAs indicated were analyzed by qPCR as in Fig. 1. Disruption of microfilaments with cytochalasin D caused minimal changes in NGF-induced axonal transport. Disrupting microtubule-based transport with colchicine completely blocked NGF-dependent changes in axonal mRNA levels, attenuating both the increase and decrease in axonal transport (*, $P \leq 0.01$; student Newman-Keul test). (B) To determine whether the NGF-dependent changes in axonal mRNA transport seen in Fig. 1 required a localized axonal source of NGF, cultures of injury-conditioned DRG neurons were exposed to 100 ng/ml NGF in solution versus exposing only the axonal compartment to immobilized NGF corresponding to a concentration of 100 ng/ml. DRG cultures exposed to NGF in solution had a distinct response compared with the immobilized NGF treatment of the axonal compartment. With the exception of vimentin, those transcripts that were increased by the local application of NGF showed significantly lower levels in response to the bath application of NGF (*, $P \leq 0.01$; student Newman-Keul test). Those transcripts decreased in response to local NGF treatment, and some that had no response to NGF showed a variable but statistically different response to bath application (**, $P \leq 0.01$; student Newman-Keul test). (A and B) Error bars represent the SD of three replicate experiments with each sample measured in quadruplicate.

shown in Table I that was comprised of five mRNAs with increased transport with NGF, five mRNAs with decreased transport with NGF, and five mRNAs with no response to NGF. The disruption of microfilaments decreased the NGF-dependent alterations in axonal mRNA levels but not to the extent that was seen with the microtubule-depolymerizing agent (Fig. 3 A). Although colchicine treatment modestly reduced overall axonal mRNA levels, the NGF-induced changes in axonal levels were almost completely abolished by colchicine (Fig. 3 A). Specificity for the effect of colchicine on NGF-dependent RNA localization is indicated by the lack of any effect of colchicine or cytochalasin D on the nonresponding mRNAs (Fig. 3 A). These observations further suggest that neurotrophins regulate axonal mRNA levels by altering the rates of transport of mRNAs from the cell body.

A change in delivery of mRNAs into axons with peripheral stimulation could require that instructive signals from the axons be retrogradely transmitted to the neuronal cell body (or nucleus). To determine whether the aforementioned alterations for mRNA levels require stimulus localized to the axonal compartment, we compared axonal mRNA levels after the application of immobilized NGF to axons versus bath-applied NGF (i.e., soluble), which would simultaneously stimulate axonal and cell body compartments. Approximately equivalent levels of soluble versus immobilized ligand were applied based on our previous assessments of TrkA phosphorylation by the NGF microparticles (Willis et al., 2005). Roughly twofold more β-actin mRNA accumulated in the axons with local stimulation than with bath-applied NGF (Fig. 3 B). Peripherin and Kv3.1a mRNAs showed no response to bath-applied neurotrophins,

Published September 4, 2007

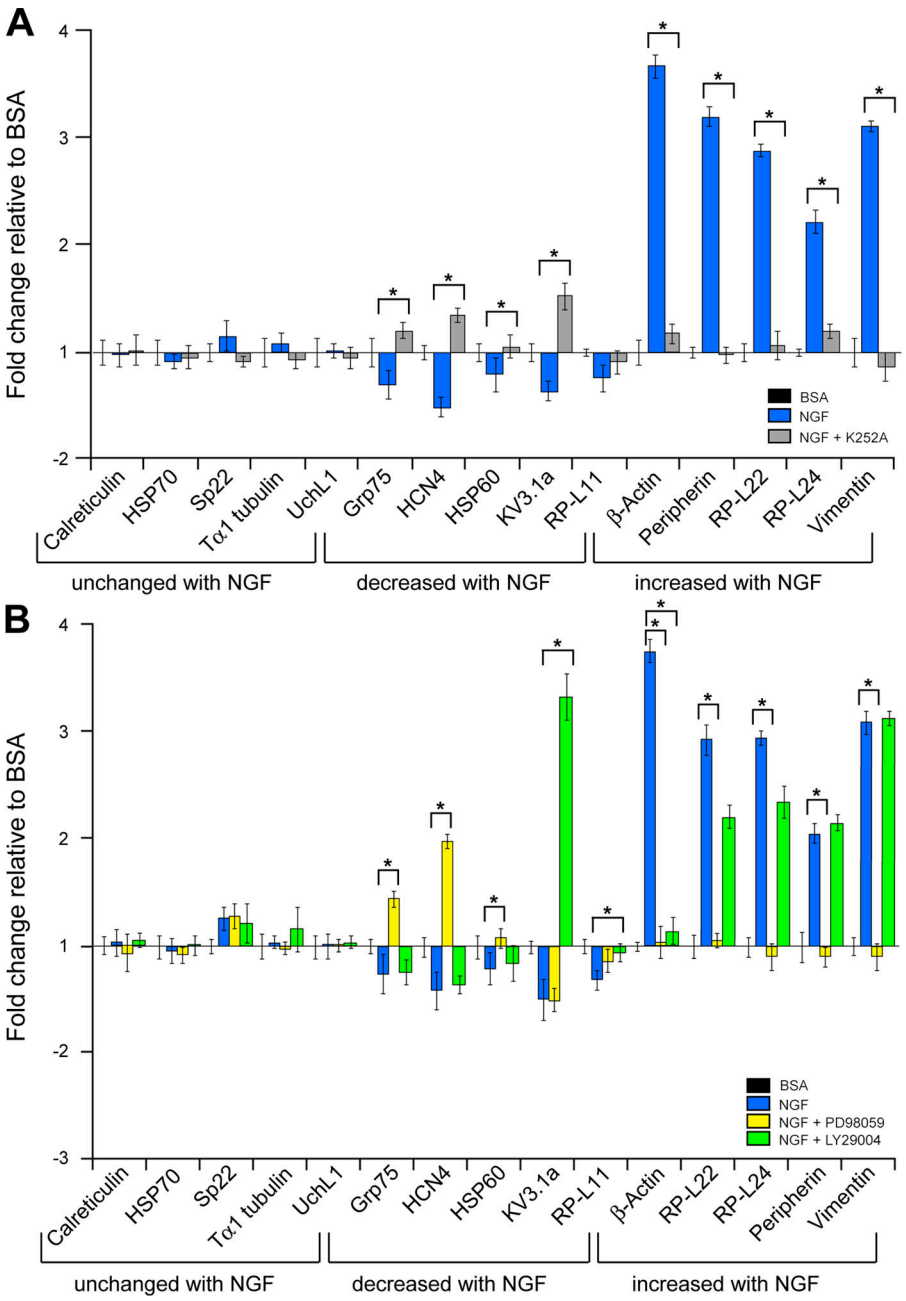

Figure 4. **Divergent signaling pathways regulate axonal mRNA levels in response to neurotrophins.** (A) Injury-conditioned DRG cultures were pretreated with 200 nM K252A to inhibit Trk tyrosine kinase activity for 30 min before application of NGF microparticles to the axonal compartment. Axonal mRNAs were analyzed by qPCR as in Fig. 1; the NGF-treated samples were normalized to the BSA control, and the K252A plus NGF-treated cultures are expressed relative to BSA plus K252A. K252A treatment altered the response to NGF microparticles, attenuating the increase in those mRNAs whose axonal levels were increased by neurotrophins. For transcripts that exhibited decreased axonal levels in response to NGF, K252A reversed the effect of NGF, resulting in increased axonal mRNA localization. (B) To evaluate signaling events downstream of TrkA, injury-conditioned DRG cultures were treated with MEK1 (PD98059) and PI3K (LY29004) inhibitors for 30 min before exposing the axonal compartment to immobilized NGF. Axonal mRNA levels were analyzed by qPCR as in Fig. 1; the NGF-treated samples are normalized to the BSA control, and the PD98059 or LY294002 plus NGF-treated cultures are expressed relative to PD98059 or LY294002 plus BSA, respectively. NGF-induced axonal localization or depletion of the majority of mRNAs was attenuated or reversed by inhibition of the MAPK pathway with PD98059. Two transcripts behaved differently. The depletion of axonal Kv3.1a mRNA by NGF was completely reversed by the inhibition of PI3K, and the increased levels of β-actin mRNA seen with NGF treatment was blocked equally well by the inhibition of MEK1 or PI3K. (A and B) Error bars represent the SD of three replicate experiments with each sample measured in quadruplicate (*, $P \leq 0.01$; student Newman-Keul test).

whereas axonal HCN4 mRNA appeared more sensitive to bath-applied NGF than localized ligand sources. With bath application of NGF, calreticulin, and HSP70 mRNAs, two transcripts that did not respond to localized NGF showed alterations in axonal mRNA levels, indicating that these transcripts uniquely respond to the soluble ligand (Fig. 3 B). Collectively, these data indicate that the stimulus derived from localized neurotrophin sources is qualitatively and quantitatively different from the nonlocalized stimulus of the soluble ligand.

Modulation of axonal mRNA localization through divergent signaling pathways

To determine the role of Trk receptors in neurotrophin-dependent axonal mRNA localization, cultures were pretreated with K252A at levels that specifically inhibit Trk tyrosine kinase activity (Tapley et al., 1992). For the mRNAs that increased with axonal NGF stimulation, K252A pretreated cultures showed axonal levels that were nearly indistinguishable from neurons exposed to control microparticles (Fig. 4 A). Axonal levels of the five nonresponding transcripts were not affected by K252A treatment (Fig. 4 A). Surprisingly, mRNAs with NGF-dependent decreases in axonal content showed a complete reversal, exhibiting increased axonal levels with Trk inhibition and peripheral NGF stimuli (Fig. 4 A). Both Kv3.1a and HCN4 mRNAs, for which levels were decreased by ~1.5-fold in the axons treated with NGF, showed a one- to twofold increase in axonal levels in cultures treated with K252A (Fig. 4 A). This indicates that local sources of NGF can signal through Trk receptors to bidirectionally modulate the axonal localization of individual mRNAs.

Published September 4, 2007

The neurotrophin-dependent activation of phosphatidyl inositol-3 kinase (PI3K) and Ras–MAPK pathways contribute to the local trophic and tropic effects of NGF and other neurotrophins (Segal, 2003). We used pretreatment with MEK1 and PI3K inhibitors (PD98059 and LY29004, respectively) to test whether these signaling pathways play a role in the neurotrophin-dependent regulation of axonal mRNA localization. The five mRNAs that previously did not respond to NGF remained unaffected overall by PD98059 and LY29004, indicating that basal activity of PI3K and MEK1 did not contribute to their axonal localization (Fig. 4 B). For most of the regulated mRNAs, NGF's effects on their axonal levels were attenuated by inhibition of the MAPK pathway with PD98059 (Fig. 4 B). However, two transcripts behaved differently. The NGF-dependent attenuation of Kv3.1a mRNA's axonal localization required PI3K activity but was unaffected by the MEK1 inhibitor (Fig. 4 B). The increased axonal localization of β-actin mRNA seen with NGF was attenuated by the inhibition of either PI3K or MEK1 (Fig. 4 B). All other mRNAs that localized in response to NGF (e.g., vimentin and peripherin) required MEK1 but not PI3K (Fig. 4 B). Thus, a single ligand can uniquely regulate the axonal localization of individual mRNAs using different downstream signaling pathways.

Focal ligand sources instruct the neuron where and where not to localize mRNAs within axons

Although extremely sensitive, the reverse transcription qPCR method used in Figs. 1–4 provides no information on where mRNAs are localized within the axon. Because axonal β-actin mRNA showed divergent regulation with growth-promoting versus growth-inhibiting stimuli and appeared more sensitive to localized ligand sources, we used the well-characterized localization elements of β-actin mRNA to drive the axonal localization of heterologous mRNAs encoding a reporter protein. For this, the 3′ untranslated region (UTR) of enhanced GFP$^{NLS/myr}$ (eGFP$^{NLS/myr}$; Aakalu et al., 2001) was replaced with 3′ UTRs from the rat β-actin or γ-actin mRNAs (eGFP$^{NLS/myr}$β-actin and eGFP$^{NLS/myr}$γ-actin, respectively). β-actin mRNA 3′ UTR contains a zipcode element that directs the transport of this mRNA in fibroblasts, myocytes, and neurons; γ-actin mRNA does not contain any similar element, and the transcript is retained in the perinuclear region (Lawrence and Singer, 1986; Kislauskis et al., 1994; Bassell et al., 1998). To facilitate expression in the adult DRG neurons, we generated adenoviruses (AVs) that express these reporter cDNAs (AV-eGFP$^{NLS/myr}$γ-actin and AV-eGFP$^{NLS/myr}$β-actin). In injury-conditioned DRG cultures infected with AV-eGFP$^{NLS/myr}$γ-actin, reporter fluorescence accumulated in the cell body and did not extend into the axonal compartment (Fig. S3, available at http://www.jcb.org/cgi/content/full/jcb.200703209/DC1). In contrast, GFP signal was seen in the cell body and at foci along the axonal processes, including the growth cones in cultures infected with AV-eGFP$^{NLS/myr}$ β-actin (Fig. S3). The myr domain of this eGFP$^{NLS/myr}$ construct likely restricts diffusion of the eGFP product in the axonal compartment, providing a measure of localized protein synthesis as previously reported (Aakalu et al., 2001). RT-PCR from axonal RNA also confirmed the differential localization of eGFP$^{NLS/myr}$ β-actin versus eGFP$^{NLS/myr}$γ-actin mRNAs in the DRG cultures (unpublished data). Thus, similar to axons of developing cortical neurons (Zhang et al., 1999; Gu et al., 2002), the 3′ UTR of β-actin mRNA is sufficient for axonal localization in adult rat sensory neurons.

Because the β-actin 3′ UTR appeared to direct axonal localization of eGFP mRNA in the DRG cultures, we next considered whether axonal localization of eGFP$^{NLS/myr}$β-actin is modulated by growth-promoting and growth-inhibiting stimuli. Analyses of axons exposed to NGF microparticles showed that GFP signals under the control of β-actin 3′ UTR accumulated directly adjacent to the ligand source during a 50-min exposure (Fig. 5 A and Video 1, available at http://www.jcb.org/cgi/content/full/jcb.200703209/DC1). Axons typically showed a sprouting or turning response upon contact with NGF microparticles (Fig. S4). BSA microparticles did not affect the intensity of GFP signals or the directionality of axonal growth (Fig. S4). At the completion of a 50-min exposure, axonal GFP fluorescence was significantly greater adjacent to NGF when compared with BSA microparticles (5.29 ± 0.07-fold for NGF vs. BSA; $P \leq 0.001$). Although there is an inherent experimental delay in when video sequences can be initiated with this approach (i.e., as the particles settle onto the coverslip), there was also a consistent increase in GFP fluorescence adjacent to NGF microparticles over the course of the imaging sequences (1.6 ± 0.09-fold for $t = 50$ vs. $t = 0$ min; $P \leq 0.001$). Similar to the effects of kinase inhibitors upon the endogenous β-actin mRNA shown in Fig. 4, the inhibition of Trk or downstream MEK1 or PI3K activity prevented any GFP accumulation adjacent to the NGF source (Figs. 5 B and S4 and Video 2). Thus, the dynamic redistribution of mRNA likely directly impacts the translation and accumulation of protein.

Microtubule-depolymerizing agents were used to determine whether an increase in GFP$^{NLS/myr}$β-actin signals was the result of RNA accumulation at NGF sources. No NGF-dependent accumulation of GFP was seen in cultures exposed to colchicine (Fig. 5 C and Video 3, available at http://www.jcb.org/cgi/content/full/jcb.200703209/DC1). The continued increase in GFP signals in the growth cone (distal to NGF source) indicates that the colchicine treatment did not affect translation of the eGFP$^{NLS/myr}$β-actin mRNA that had already accumulated in the growth cone. Because colchicine completely blocked NGF-dependent increases in axonal β-actin mRNA levels in the qPCR experiments (Fig. 3 A), the majority of the increased GFP signals shown in Fig. 5 A can be attributed to the subcellular localization of eGFP$^{NLS/myr}$β-actin mRNA rather than to the translational activation of any eGFP$^{NLS/myr}$β-actin mRNA already residing within the axon.

Because microtubule depolymerization would alter both retrograde and anterograde transport, we tested whether the NGF effect on eGFP$^{NLS/myr}$β-actin required retrograde signaling. For this, DRG cultures were transfected with dynein heavy chain (Dync1h1) siRNAs (He et al., 2005). The transfected cultures showed a decrease of Dync1h1 protein, and transfected neurons showed a selective depletion of retrograde but not anterograde transport (Fig. S2 B and Video 4, available at

Published September 4, 2007

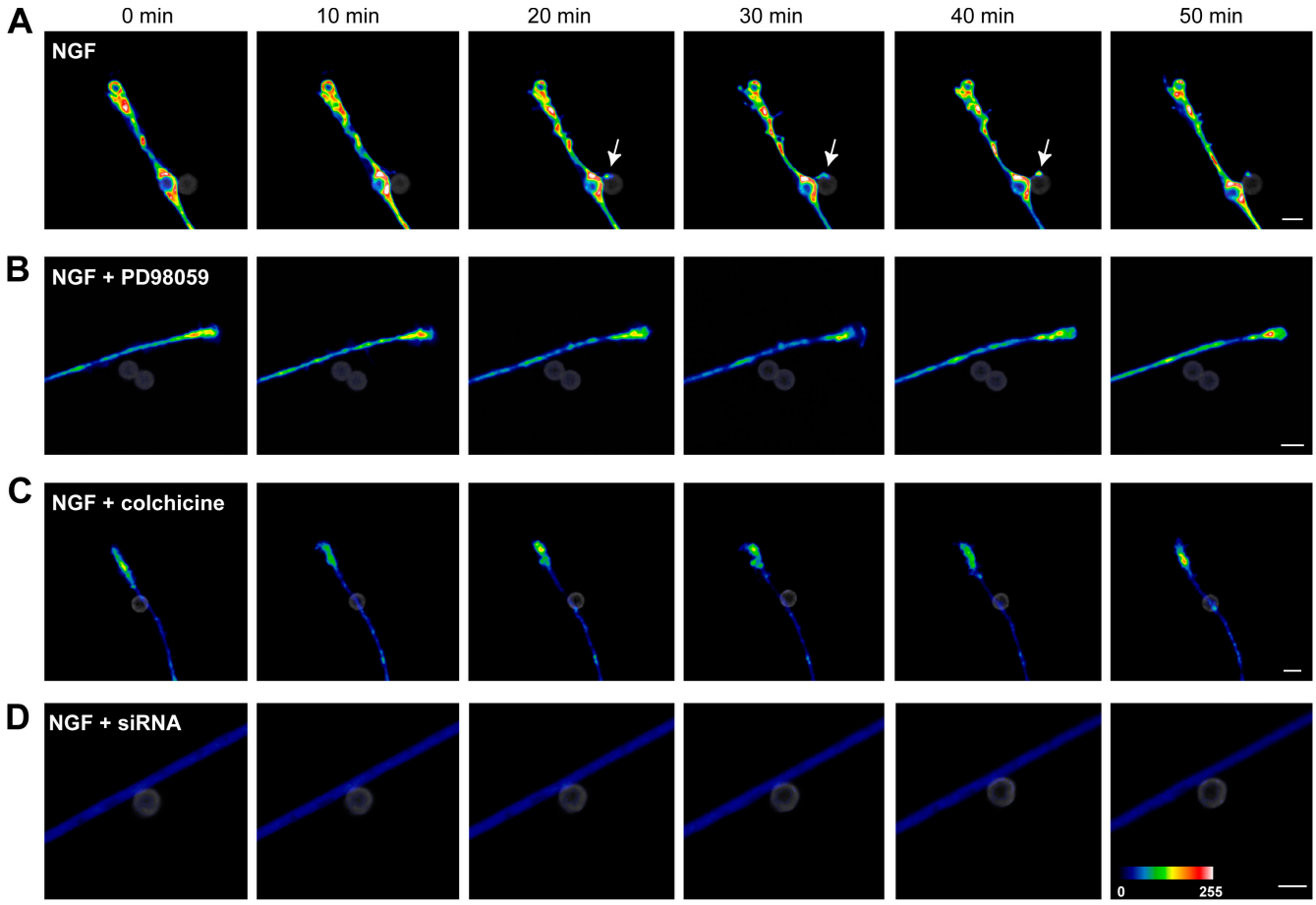

Figure 5. **eGFP$^{NLS/myr}$β-actin translation product accumulates adjacent to NGF sources through instructive changes in the localization of its mRNA.** Naive DRG cultures were infected with AV-eGFP$^{NLS/myr}$β-actin and exposed to NGF microparticles (gray) after 2 d in culture. The images show GFP signal from confocal images through the distal axon collected beginning ~20 min after ligand addition (to allow the microparticles to settle) and continuing for 50 min of live cell imaging with images collected at 1-min intervals. Still images at 10-min intervals are shown. GFP signal is displayed as a spectrum, as indicated in the final panel of sequence C. (A) NGF microparticles caused GFP signal accumulation directly adjacent to the NGF stimulus (Video 1, available at http://www.jcb.org/cgi/content/full/jcb.200703209/DC1). In the latter portions of the sequence, a branch point with intense GFP signal can be seen directly adjacent to the microparticle (arrows). (B) Pretreatment with PD98059 prevented any change in GFP signal intensity at the site of contact with the NGF microparticle (Video 2). (C) Treatment with colchicine attenuated any change in GFP signal intensity adjacent to NGF microparticles compared with A (Video 3). (D) DRG cultures treated with dync1h1 siRNA showed decreased retrograde transport of LysoTracker dye (Video 4) and no change in GFP signal over a 50-min exposure to NGF microparticles. The images shown here are representative of at least 30 observations per condition with ≥80% concordance between experimental observations. Bars, 5 μm.

http://www.jcb.org/cgi/content/full/jcb.200703209/DC1). These siRNA-transfected neurons also showed no significant alteration ($P > 0.05$) in eGFP$^{NLS/myr}$β-actin signals over 50 min of exposure to NGF microparticles (0.91 ± 0.11-fold for NGF vs. BSA; Fig. 5 D). DRG cultures treated with erythro-9-(2-hydroxy-3-nonyl)adenine hydrochloride (EHNA), which has been shown to inhibit dynein ATPase activity (Ekstrom and Kanje, 1984; Shpetner et al., 1988), had similar depletion of retrograde transport (Video 5) and showed no significant change ($P > 0.05$) in axonal GFP fluorescence in response to NGF (0.95 ± 0.10-fold for NGF vs. BSA). Thus, the NGF-dependent increase in localization of the axonal reporter mRNA appears to require retrograde transport.

To determine how growth-inhibiting stimuli can deplete axonal β-actin mRNA levels, we examined the effect of immobilized MAG on axonal GFP signals in AV-eGFP$^{NLS/myr}$β-actin–infected DRG cultures. GFP signals were relatively excluded from axonal regions adjacent to MAG sources (Fig. 6 A and Video 6, available at http://www.jcb.org/cgi/content/full/jcb.200703209/DC1) and often caused the axon to turn away from the MAG source (Fig. S4). After 50-min exposure to microparticles, GFP signals were significantly decreased with MAG-Fc microparticles when compared with the control IgG Fc microparticles (0.68 ± 0.1-fold for MAG-Fc vs. IgG Fc; $P \leq 0.001$). The eGFP$^{NLS/myr}$β-actin translation product was relatively depleted from the vicinity of MAG-Fc (Fig. S4); this focal exclusion of GFP adjacent to MAG sources is likely why MAG caused only a small reduction in β-actin mRNA by qPCR. In contrast to NGF's effects on eGFP$^{NLS/myr}$β-actin signals, a statistically significant attenuation of axonal GFP signals adjacent to MAG stimuli was still seen when retrograde transport was inhibited with Dync1h1 siRNA (0.75 ± 0.07-fold for MAG vs. IgG Fc; $P \leq 0.01$; Fig. 6 B) or EHNA (0.73 ± 0.12-fold for MAG vs. IgG Fc; $P \leq 0.01$; not depicted). Thus, the MAG-dependent depletion of GFP signals appeared to be a local effect adjacent to axonal stimuli.

Published September 4, 2007

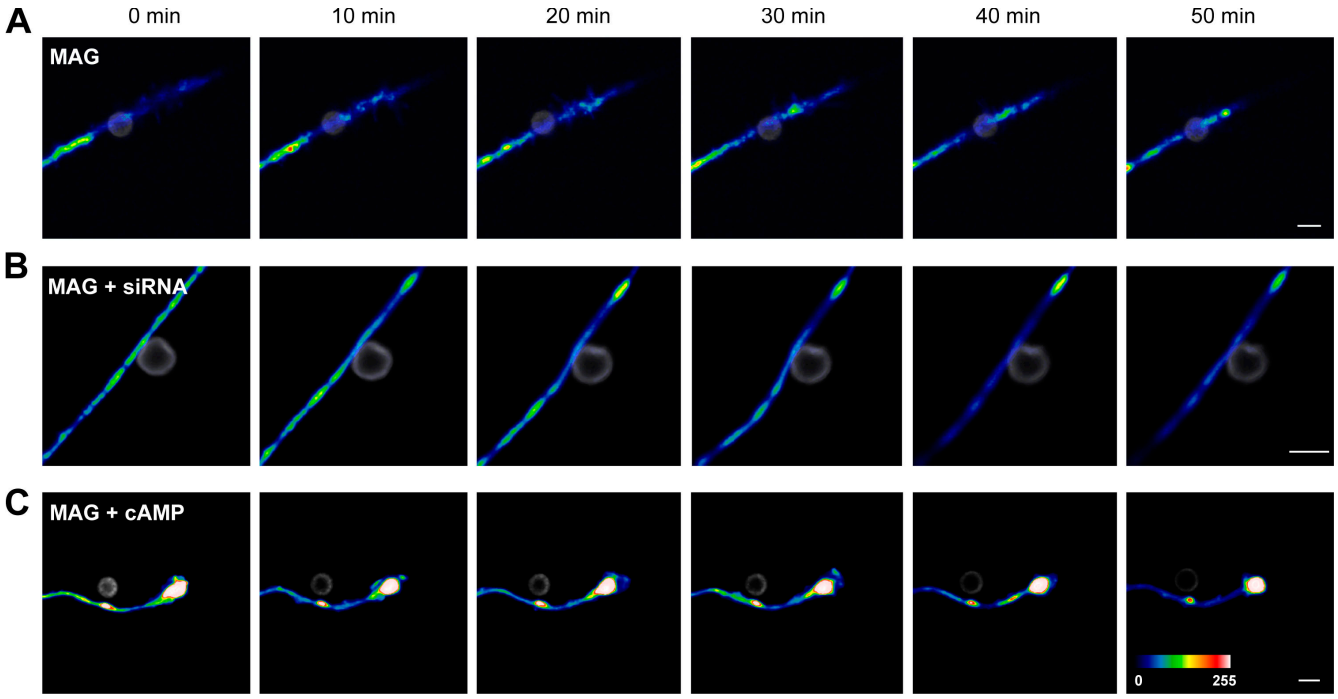

Figure 6. **eGFP$^{NLS/myr}$β-actin translation product is relatively excluded from regions adjacent to MAG sources.** Naive DRG cultures were infected with AVeGFP$^{NLS/myr}$β-actin as in Fig. 5. After 2 d, cultures were exposed to MAG microparticles. Image sequences were acquired for the indicated intervals beginning at 20 min after the addition of microparticles. GFP signal is displayed as a spectrum (see final panel in series B). (A) DRGs exposed to MAG microparticles show the exclusion of GFP signal adjacent to MAG stimulus. Coincident with the decrease in eGFP$^{NLS/myr}$β-actin mRNA translation, the axon begins to retract upon contact with the MAG microparticle (Video 6, available at http://www.jcb.org/cgi/content/full/jcb.200703209/DC1). (B) In dync1h1 siRNA-treated cultures, focal sources of MAG resulted in a decrease in GFP signal over the 50-min video sequence. (C) Pretreatment with db-cAMP reversed the response to MAG microparticles with an accumulation of GFP directly adjacent to the MAG (Video 7). The images shown here are representative of at least 30 observations per condition with ≥ 80% concordance between experimental observations. Bars, 5 μm.

The growth-inhibitory effects of MAG can be overcome by elevating neuronal cAMP levels (Cai et al., 1999, 2001; Neumann et al., 2002). To determine whether the MAG-dependent changes in the localized production of eGFP$^{NLS/myr}$β-actin could be altered by cAMP, cultures were treated with a cell-permeable nonhydrolyzable cAMP analogue (dibutyral cAMP [db-cAMP]) before exposure of axons to immobilized MAG. In db-cAMP–treated cultures, eGFP$^{NLS/myr}$β-actin signals accumulated directly adjacent to the MAG microparticles (Fig. 6 C and Video 7, available at http://www.jcb.org/cgi/content/full/jcb.200703209/DC1). The GFP signals showed a significant increase adjacent to MAG-Fc microparticles after cAMP treatment when compared with IgG Fc control (4.47 ± 0.06-fold for MAG-Fc + db-cAMP vs. IgG Fc + db-cAMP; $P \leq 0.001$), and, similar to the NGF response, axons turned acutely after contact with the MAG microparticles (Fig. S4). Pretreatment with db-cAMP did not alter the response seen by contact with NGF or control microparticles (unpublished data).

Ligand-dependent localization of endogenous axonal mRNAs

FISH was used to determine whether focal stimulation of axons with growth-promoting versus growth-inhibiting ligands could similarly alter the local accumulation of endogenous mRNAs in these axons. For this, injury-conditioned DRGs were plated onto laminin-coated coverslips with adherent neurotrophin, MAG, and Sema3A microparticles. After 18 h in culture, cells were fixed and analyzed by FISH for mRNA and immunofluorescence for neurofilament. Differences in mRNA signal intensity adjacent to the immobilized agent were specific both at the level of the transcript and ligand. Consistent with the transfected eGFP$^{NLS/myr}$β-actin, endogenous β-actin mRNA was enriched adjacent to neurotrophin sources and decreased adjacent to MAG and Sema3A sources (Fig. 7 A). The disparity between the responses elicited by NGF and NT3 seen in the qPCR experiments for peripherin and Kv3.1a mRNAs was also evident in the localization of these transcripts along axons exposed to immobilized NGF and NT3. Peripherin mRNA increased at the site of NGF stimuli but decreased adjacent to NT3 stimuli (Fig. 7 B). The opposite pattern was seen with Kv3.1a mRNA: FISH signals for Kv3.1a were decreased adjacent to NGF stimuli but increased adjacent to NT3 stimuli (Fig. 7 C). Together, these findings show that the exquisite ligand specificity for mRNA localization seen in the qPCR experiments corresponded to localized accumulation or depletion of individual transcripts directly at the site of ligand exposure.

Discussion

Targeting mRNAs and translational machinery to subcellular loci is being increasingly recognized as a means to locally control the protein composition of cellular domains. Modulating the levels

Published September 4, 2007

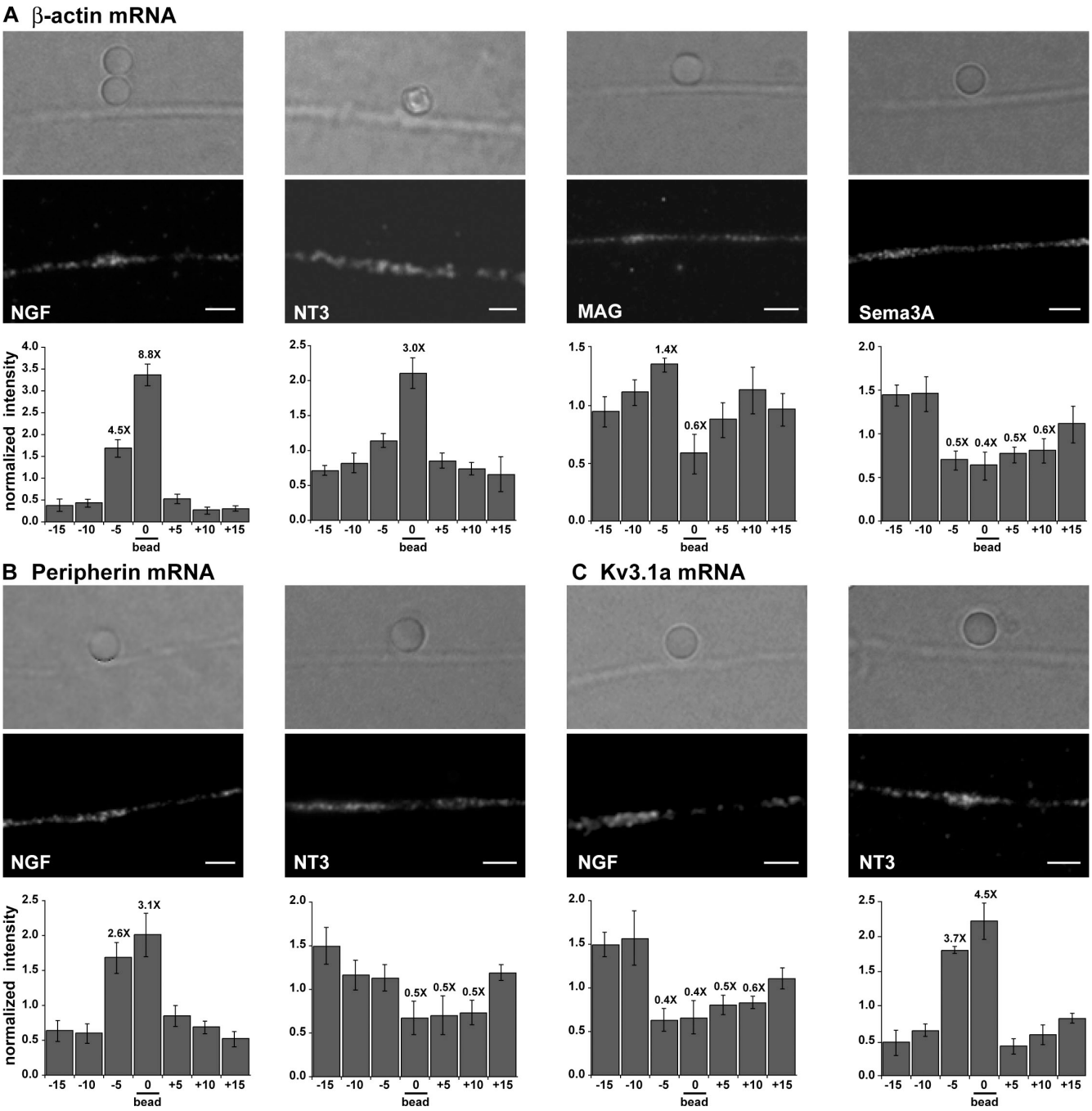

Figure 7. **Axonal mRNA levels are altered at the site of tropic stimulation.** (A–C) Injury-conditioned DRGs were grown in the presence of focal immobilized sources of attractive or repulsive chemotropic agents for 18 h and analyzed by FISH for β-actin (A), peripherin (B), or Kv3.1a mRNA (C). Representative differential interference contrast and fluorescent signals for mRNAs are illustrated for each indicated condition. The DRG processes were visualized by immunofluorescence for neurofilament heavy subunit (not depicted). The differential interference contrast images are focused on the microparticle to show the bead position relative to the axon. The bar graphs show relative axonal mRNA signal intensity in 5-μm bins that were normalized to the mean signal intensity across the axon (an x-axis value of 0 indicates the 5-μm bin that bisected the microparticle; proximal negative numbers indicate the proximal axon, and positive numbers indicate the distal axon). Quantitative data were obtained from three separate experiments, and error bars represent the SD of 30 individual axons measured over these repetitions by a blinded observer. Fold differences are indicated in bins that are significantly different compared with the most proximal segment ($P \leq 0.01$; student Newman-Keul test). Bars, 5 μm.

of individual mRNAs in different subcellular regions could alter the populations of proteins generated in these regions by locally altering the availability of templates for the local translational machinery. Because of the distances separating neuronal processes from their cell body, neurons are an appealing cellular model for testing how local stimuli alter the trafficking of mRNAs into subcellular regions. Both the dendritic and axonal compartments of neurons have been used to study the localization of single transcripts, but the specificity of such changes has not been addressed for a broad population of mRNAs. Localized protein

Published September 4, 2007

synthesis has been shown to provide a means for axons to autonomously respond to guidance cues and injury (Willis and Twiss, 2006). Studies showing altered translation in axons have either not provided any analyses of which proteins are locally generated or have focused on single proteins (Wu et al., 2003; Piper and Holt, 2004; Wu et al., 2005; Leung et al., 2006; Piper et al., 2006; Yao et al., 2006). In the present study, we show that both growth-promoting and growth-inhibiting stimuli can differentially localize mRNAs to points of ligand stimulation.

The specificity in these mRNA localization responses is exhibited at multiple levels, including differential responses to growth-promoting versus growth-inhibiting ligands, differential responses to individual growth-promoting ligands, and even differences within downstream signaling pathways for responses to an individual ligand. The microtubule-dependent changes in axonal mRNA levels were reflected by a reciprocal decrease or increase in cell body mRNA content, suggesting a ligand-dependent alteration in delivery of mRNAs from the cell body. However, our data do not completely exclude the possibility that localized mRNA stability may also contribute to axonal mRNA content. Likewise, it is possible that both mRNA transport and stability are affected by distinct signaling pathways. Regardless of the specific mechanism, our findings indicate that extracellular signals can change the local concentrations of axonal mRNAs, which likely provides unique specificity to the localized protein synthetic responses.

Modulation of axonal mRNA levels is ligand specific

Although neurotrophins have been shown to increase the axonal localization of β-actin mRNA and local application of NGF and BDNF increases axonal levels of peripherin and vimentin mRNAs (Zhang et al., 1999, 2001; Willis et al., 2005), it has not been clear whether the neurotrophins or other ligands can decrease the axonal localization of any mRNAs. By analyzing the axonal levels of a large panel of mRNAs, our study shows that the axonal localization of individual mRNAs can be specifically increased or decreased in response to different ligands. A localized redistribution of mRNAs within the axons could contribute to the focal depletion of mRNAs as well as the translation product of localized $eGFP^{NLS/myr}$β-actin mRNA adjacent to stimuli. With recent observations of the asymmetric redistribution of mRNA within growth cones in response to ligands (Leung et al., 2006; Yao et al., 2006) and the known short-range and bidirectional movements of RNA-binding proteins within RNA processes (Kiebler and Bassell, 2006), it is tempting to speculate that retrograde movement of mRNAs may also contribute to the decreased axonal mRNA levels seen in the quantitative experiments used here. Thus, although the reverse transcription qPCR approach has given us a unique view of dynamic ligand-dependent changes in total axonal mRNA levels, further studies will be needed to fully dissect the contributions of mRNA degradation and retrograde movement within axons for determining localized mRNA levels.

Surprisingly, even when ligands induce similar trophic responses, as with the individual neurotrophins, particular mRNAs can be uniquely affected. NGF and BDNF showed overall similar changes in levels of individual axonal mRNAs, but the response to NT3 appeared distinct. It is intriguing to speculate that differences in RNA transport reflect effects of these neurotrophins acting upon different neuronal subpopulations in the DRG (Snider, 1994). The ubiquitous expression of some mRNAs tested here (e.g., ribosomal proteins L22, L24, and S17;Amaldi et al., 1989; Kaspar et al., 1993) argues that these transcripts should also be available for regulation in the NT3-responsive DRG neurons. The extensive overlap between NGF, BDNF, and NT3 signal transduction (Segal, 2003) suggests that mRNA localization is matched to the specific ligand rather the overall trophic or tropic response to that ligand. Despite this overlap, tropic responses to neurotrophins can be distinct because cAMP can modify turning responses to NGF and BDNF, whereas cyclic guanosine monophosphate can modify turning responses to NT3 (Song and Poo, 1999). However, even with the similarities between NGF and BDNF, axonal levels of GAP-43 mRNA were uniquely altered by NGF. Because GAP-43 is expressed by all DRG neurons in the injury-conditioned cultures that were used here (Chong et al., 1994; Smith and Skene, 1997), GAP-43 mRNA should certainly be available for regulation in the BDNF-responsive neurons.

Ligand-specific effects were not limited to growth-promoting stimuli because DRG cultures treated with Sema3A and MAG also showed altered levels of individual mRNAs in the axons. Both the semaphorins and myelin inhibitors cause growth cone retraction in DRG neurons (Tanelian et al., 1997; Tang et al., 2001). For all but one of the 50 transcripts tested (vimentin), Sema3A and MAG modulated the localization of different mRNAs or generated the opposite response for individual mRNAs when compared with the neurotrophins. This supports the concept that axonal mRNA localization is tightly regulated with peripheral stimuli uniquely targeting individual mRNAs for focal increase or decrease along the axon.

Signal transduction pathways regulating axonal mRNA localization

Analyses of intracellular signaling showed further evidence of specificity for axonal mRNA localization mechanisms. Activation of Src family tyrosine kinases and Cdks by Sema3A increases rates of retrograde and anterograde vesicular transport even in isolated axons, but it is not clear what cargo is being transported in response to Sema3A (Sasaki et al., 2002; Li et al., 2004). Our data suggest that the local Sema3A stimulation of axons can direct the anterograde transport of cargo that includes mRNAs. The Sema3A-induced changes in axonal mRNA levels were sensitive to inhibition of Src family tyrosine kinases and Cdks (unpublished data), which is similar to what has been demonstrated for Sema3A-dependent vesicular transport (Sasaki et al., 2002; Li et al., 2004).

The neurotrophin-dependent alterations in mRNA localization reported here are Trk dependent for both the positively and negatively regulated mRNAs. For NGF, accumulation of the GFP reporter mRNA required retrograde transport. Although Trk activation is an obligate step in initiating retrograde signaling, there has been some debate about whether Trk is internalized and whether the retrogradely transported Trk includes ligand (Campenot and MacInnis, 2004; Zweifel et al., 2005). Our data do not distinguish whether Trk internalization is required for

Published September 4, 2007

altering mRNA localization. We cannot completely exclude that NGF is not leached from the microparticles even with the covalently bound ligands used here; however, we were previously unable to detect the release of noncovalently bound NGF from microparticles over the 4-h incubation period used in this study (Willis et al., 2005). Moreover, RNA localization changes seen with the local application of NGF to axons was qualitatively and quantitatively distinct from those seen with bath-applied NGF. Regardless of whether Trk and NGF internalize, our study argues that PI3K and MEK1 signaling cascades can uniquely regulate axonal mRNA localization. Because the NGF-dependent increase in β-actin mRNA was attenuated by the inhibition of Trk, PI3K, or MEK1, the neurotrophin's regulation of β-actin mRNA localization requires the sequential or convergent activation of PI3K and MEK1. The response of most other mRNAs to the neurotrophins was purely MEK1. Together, these data indicate that both divergent and convergent or sequential signaling cascades can specifically control the local concentration of mRNAs into the axonal compartment. Although we clearly detected differences between localized and bath-applied neurotrophins, we have not distinguished whether the kinase activation occurs locally within axons or in the cell body. When axonal mRNA targeting versus locally concentrating mRNAs at sites of stimulation is considered, one can hypothesize that PI3K and MEK1 may regulate the expression and/or activity of RNA-binding proteins needed for transport or docking of mRNAs and RNA granules.

Targeting mRNAs for axonal transport

The cDNA array analyses for identification of axonal transcripts show that >200 individual mRNAs can extend into these mammalian DRG processes. It is obvious that not all neuronal mRNAs extend into the axonal compartment of the cultured DRG neurons used here. This implies that the neuron somehow knows which mRNAs to target for localization into these processes. For rat β-actin mRNA, the 3′ UTR containing the rat zipcode element is sufficient to target a heterologous mRNA into adult DRG axons, similar to what has been demonstrated in other cell types (Hill et al., 1994; Kislauskis et al., 1994; Ross et al., 1997; Zhang et al., 1999; Farina et al., 2003). The other axonal mRNAs analyzed here likely contain localization elements, but their 3′ UTRs do not show any clear primary sequence homology to the β-actin zipcode (unpublished data). Interestingly, our data indicate that the DRG neurons not only know where to target mRNAs but also can be specifically instructed where not to send individual mRNAs within the axon. The localization of mRNAs to focal sites of ligand stimulation is quite similar to dendritic mRNA localization, in which activated postsynaptic regions are tagged for RNA delivery (Steward et al., 1998; Steward and Halpain, 1999; Aakalu et al., 2001; Tongiorgi et al., 2004).

Several lines of evidence indicate that localized mRNAs are also translationally regulated. Huttelmaier et al. (2005) showed that Src-dependent phosphorylation releases the zipcode binding protein from β-actin's zipcode element, allowing translational activation of the mRNA. Because microtubule depolymerization completely blocked neurotrophin-dependent increase in β-actin mRNA by qPCR and prevented the localization of $GFP^{NLS/myr}$β-actin in response to NGF, our studies suggest that localization of the encoding mRNA provides a key means to regulate axonal expression of this protein in DRG neurons. Our data do not preclude the possibility that the translation of axonal mRNAs is also tightly regulated by extracellular stimuli. This may indeed be the case for the majority of mRNAs with constitutive axonal localization.

Verma et al. (2005) reported that the ability to regenerate axons correlates with the protein synthetic capacity of the axon. Our analyses of growth-promoting and growth-inhibiting ligands suggest that the synthetic capacity of growing axons is directly regulated by extracellular stimuli. The distinct effects of the neurotrophins versus MAG and Sema3A may point to antagonistic effects of these growth-promoting and growth-inhibiting stimuli on axonal mRNA levels. The growth-inhibitory effects of MAG can be overcome by priming neurons with neurotrophins or agents that increase cAMP levels (Cai et al., 1999, 2001; Lu et al., 2004). Our data clearly show that growth-inhibiting stimuli from the central nervous system can regulate axonal mRNA localization and that these effects can be mitigated by offering the neuron antagonizing stimuli. Because MAG is a known growth inhibitory molecule in central nervous system white matter (Filbin, 2003), this raises the intriguing possibility that alterations in mRNA localization may accompany the failed regeneration of central nervous system axons. Our identification of the positive roles of neurotrophins in stimulating mRNA localization in these regenerating adult sensory neurons in vitro should provide motivation to investigate a role for similar pathways in vivo. For example, TrkB signaling can enhance axonal regeneration in vivo (English et al., 2005), and this may depend, in part, on regulated mRNA localization and localized protein synthesis in regenerating sensory and motor nerves. The effect of MAG for focal depletion of axonal β-actin mRNA did not require retrograde transport; thus, tropic stimuli that can signal the cell body to modulate axonal mRNA levels may be able to overcome the local inhibitory effects of MAG on axonal protein synthesis.

Materials and methods

Pharmacological reagents

NGF (Harlan), BDNF, NT3 (Alomone Labs), MAG-Fc (R&D Systems), and Sema3A-AP (Nakajima et al., 2006) were covalently coupled to 15-μm-diameter polystyrene microparticles according to the manufacturer's instructions (Polysciences). The following control proteins were also immobilized onto polystyrene microparticles or particles: BSA (Sigma-Aldrich) for NGF, BDNF, and NT3; human IgG-Fc (R&D Systems) for MAG-Fc; and AP for Sema3A-AP (provided by Y. Goshima, Yokohama University, Yokohama, Japan; Nakajima et al., 2006). Efficiency of absorption was determined by Bradford assay for unbound protein. To determine the mechanisms involved in modulation of axonal mRNA transport, DRG cultures were treated with the following pharmacological agents 30 min before the addition of immobilized ligands: 200 nM K252A (Calbiochem), 50 μM PD98059 (Biomol), 50 μM LY294002 (Biomol), 10 μM Lavendustin (Biomol), 10 μM Olomucine (Biomol), 1 mM db-cAMP (Sigma-Aldrich), 10 μg/ml cycloheximide (Sigma-Aldrich), 10 μM cytochalasin D (Sigma-Aldrich), and 1 μg/ml colchicine (Sigma-Aldrich). 50 nM EHNA (Sigma-Aldrich) was added to cultures 3 h before use.

Cell culture and axonal isolations

All animal surgeries and euthanasia were performed according to institutional Animal Care and Use Committee guidelines under approved protocols. Primary DRG cultures were prepared from Sprague Dawley rats that had been injury conditioned 7 d before by sciatic nerve crush at midthigh level (Smith and Skene, 1997). Dissociated cultures were prepared from

Published September 4, 2007

L4-L5 DRGs as previously described (Twiss et al., 2000). Cultures were plated at moderate density on membrane inserts (for axonal isolation, see next paragraph) or at low density on coverslips (for live cell imaging and FISH analyses, see respective sections below).

The culture method for isolating DRG axons from cell bodies and nonneuronal cells has been previously described (Zheng et al., 2001; Willis et al., 2005). In brief, dissociated DRGs were plated into tissue culture inserts containing porous membranes (8-μm-diameter pores; BD Falcon), which were coated with poly-L-lysine (Sigma-Aldrich) and laminin (Upstate Biotechnology). Axons were isolated after 16–20 h in culture by scraping away the cellular content from the upper or lower membrane surfaces (yielding axonal or cell body preparations, respectively). The purity of the axonal preparations was tested by RT-PCR for microtubule-associated protein 2, γ-actin, and β-actin mRNAs.

cDNA array analyses

Axonal RNA was isolated as described in the previous section, and the purity was confirmed by RT-PCR for β-actin, γ-actin, and microtubule-associated protein 2 (Fig. S1 A). 200 ng was used as a template for RT-PCR using the SMART PCR cDNA Synthesis kit (CLONTECH Laboratories, Inc.) to generate full-length double-stranded cDNA. Aliquots of the amplification were removed from the PCR every third cycle from 12–30 cycles and used for Southern blotting. Southern blots were probed with ^{32}P-labeled β-actin cDNA to test for linearity (Fig. S1 B). The aliquot below where linearity was lost was used to generate a ^{33}P-labeled probe cDNA using the Advantage 2 PCR System (CLONTECH Laboratories, Inc.) and hybridized to Atlas Plastic Rat 4K Microarrays (CLONTECH Laboratories, Inc.). Hybridization signals were detected by phosphorimaging, and results were analyzed using Atlas Image 2.7 software (CLONTECH Laboratories, Inc.). For comparison between arrays, individual hits were normalized across the individual array and assigned a relative intensity.

Localized treatment of axons

The culture method for treatment of intact DRG axons has been previously described (Willis et al., 2005). In brief, DRGs were cultured on a porous membrane in the presence of 80 μM of the RNA synthesis inhibitor DRB throughout the culture period (Sigma-Aldrich). After 16–20 h in culture, the axonal compartments were selectively exposed to the protein-coupled microparticles by placing the inserts into dishes with shallower wells in which the bottom surface of the insert directly contacted coated microparticles along the bottom of the wells. Microparticles of 15 μm diameter were used for these stimulations to restrict any passage through the 8-μm pores of the membrane, which limited stimulation to the axonal compartment. After 4 h of treatment, membranes were rinsed in PBS, and the axonal compartment was isolated as described in Cell culture and axonal isolations. RNA was extracted from the fractionated cultures using the RNAqueous Micro kit (Ambion) and quantified using fluorometry with the RiboGreen reagent (Invitrogen). To normalize the axonal mass between samples, flow through from the affinity-based RNA isolation was used to measure the protein content of the axonal samples by fluorometry with the NanoOrange reagent (Invitrogen). All axonal RNA samples were normalized to protein content before RT-PCR analyses (Willis et al., 2005).

To visualize the localized effects of immobilized ligand exposure to axons, 4.5-μm microparticles were used. For live cell imaging (see Live cell imaging section below), fluorescent microparticles were added to cultures growing on poly-L-lysine/laminin chambered coverslips. For the FISH studies (see FISH section below), 7-d injury-conditioned DRGs were cultured overnight in the presence of carboxylated polystyrene microparticles with immobilized neurotrophins, MAG, or Sema3A. In these experiments, the ligand-immobilized microparticles were coupled directly to the laminin surface, which prevented them from being washed away in subsequent FISH/immunofluorescence steps. For this, ligands were coupled to microparticles overnight according to the manufacturer's protocol (Polysciences). Microparticles were then added to the coated coverslips for 4 h. Unreacted sites were blocked with ethanolamine, and coverslips were washed and used for standard DRG culture.

Analysis of axonal RNAs

For analyses of axonal transcripts, normalized axonal RNAs (~50 ng each) were used as a template for reverse transcription using the iScript RT kit (Bio-Rad Laboratories). The reverse transcription reactions were diluted 10-fold, and the purity of each axonal preparation was assessed by RT-PCR for γ-actin and microtubule-associated protein 2 mRNAs, which are expressed at high levels in rat DRG cultures but are excluded from the axonal compartment as previously described (Willis et al., 2005). Validated axonal RNA preparations were then used for reverse transcription qPCR. In brief, reverse-transcribed axonal RNA was amplified using the Prism 7900HT sequence detection system (Applied Biosystems) with 2× SybrGreen Master Mix (QIAGEN) according to the manufacturer's standard cycling parameters. Rat brain RNA was used as a template to generate standard curves for all primer pairs. A robotic system (Biomek 2000; Beckman Coulter) was used to standardize the pipetting of samples and reagents into 384-well plates for qPCR. All samples were assayed in quadruplicate from at least three independent experiments each. In addition to controlling for axonal number based on protein content, the relative levels of each transcript were normalized to the 12S mitochondrial ribosomal RNA control by the comparative threshold method (C_t) to provide an internal control for reverse transcription efficiency and axonal content. RNA values are expressed relative to control (BSA for NGF, BDNF, and NT3 treatments; Fc for MAG-Fc treatment; and AP for Sema3A treatment).

Metabolic labeling of RNA

Injury-conditioned DRGs were cultured overnight ± 80 μM DRB. Culture medium was then supplemented with 125 mCi/ml α-[^{32}P]UTP (GE Healthcare). After a 4-h labeling period, total RNA was extracted and quantified by fluorometry as described in Localized treatment of axons. The specific activity was determined by liquid scintillation counting. These labeled RNA samples (2 μg each) were electrophoresed in a 6% acrylamide gel. After electrophoresis, the gel was stained with ethidium bromide, imaged under UV to verify RNA loading and integrity, dried, and used for autoradiography.

cDNA constructs for expressing chimeric mRNAs

Chimeric reporter cDNA constructs were generated by replacing the 3′ UTR of the αCamKII-eGFP$^{NLS/myr}$ constructs (provided by E. Schuman, California Institute of Technology, Pasadena, CA; Aakalu et al., 2001) with that of the rat γ-actin and β-actin mRNAs. cDNA encoding 3′ UTRs of these rat mRNAs were isolated by RT-PCR from rat brain RNA template using the following primers engineered with Not1 and Xh1 restriction sites (actin components are underlined): sense β-actin (5′-AAGGAAAAAAGCGGCCGCGCGGACTGTTACTGAGCTGCG-3′), antisense β-actin (5′-TTTAACTCGAGTTTATTCGGTCTCACGTCAGT-3′), sense γ-actin (5′-AAGGAAAAAAGCGGCCGCGCAGATGGACTGAGCAGGTGCCAGG-3′), and antisense γ-actin (5′-TTTAACTCGAGCTTTTATTTCTCTTTACACAAT-3′). PCR products were cloned into pTOPO vector (Invitrogen) and sequenced. Sequences were compared with γ-actin and β-actin 3′ UTRs published in GenBank; verified cDNA inserts were subcloned into the eGFP construct to generate peGFP$^{NLS/myr}$γ-actin and peGFP$^{NLS/myr}$β-actin. These plasmids were tested for expression and subcellular localization of the encoded eGFP by transfecting naive DRG cultures using LipofectAMINE 2000 (Invitrogen). Once validated, the eGFP$^{NLS/myr}$ plus 3′ UTR cassettes were digested with Nru1 and Xho1 and subcloned into Pme1 and Xho1 sites of pVQ-CMV-kNpA shuttle plasmid (Viraquest) for the generation of AV. The in vitro recombination and generation as well as packaging and titering of AVeGFP$^{NLS/myr}$γ-actin and AVeGFP$^{NLS/myr}$β-actin were provided as a fee for service (Viraquest).

For adenoviral-based expression, dissociated DRG neurons were exposed to 150 MOI AVeGFP$^{NLS/myr}$β-actin or AVeGFP$^{NLS/myr}$γ-actin for 15 min at 37°C after the last trituration step in dissociating DRGs for culture. Cultures were plated onto chambered coverglass (Nalgene) coated with poly-L-lysine and laminin. Cultures were grown for 16–20 h when ≥70% of cells showed GFP expression.

siRNA transfection

Dynein-based transport was diminished using ON-TARGET Plus SMARTpool siRNA targeting Dync1h1 (GenBank/EMBL/DDBJ accession no. NM_019226; Dharmacon). siGLO-Red reagent (Dharmacon) was used for identifying transfected neurons in the live cell imaging experiments (see Live cell imaging section below). After 12 h in vitro, DRG cultures were transfected with siRNAs using DharmaFECT3 as per the manufacturer's instructions (Dharmacon). The cultures were exposed to 50 nM of total siRNA (25 nM Dync1h1 and 25 nM siGLO-Red) plus 1.0 μl DharmaFECT3 in a total culture volume of 1 ml. After 24 h, the culture medium was replaced, and the cells were allowed to grow for 72 h.

Effectiveness of the siRNAs for depleting Dync1h1 was analyzed by immunoblotting

For this, control and siRNA-treated cultures were lysed in radioimmunoprecipitation assay buffer (0.1% SDS, 50 mM Tris-Cl, pH 6.8, 150 mM NaCl, 0.5% NP-40, and 2 mM EDTA), cleared by centrifugation, and normalized for protein content by Bradford assay (Bio-Rad Laboratories). Lysate were denatured, fractionated by SDS/PAGE, and transferred to polyvinylidene

Published September 4, 2007

difluoride membrane (Willis et al., 2005). Blots were blocked in Tris-buffered saline with 0.1% Tween 20 (TBST) plus 5% nonfat dry milk for 1 h and then incubated overnight at 4°C in rabbit anti–dynein HC antibody (1:200; Santa Cruz Biotechnology, Inc.). Blots were rinsed several times in TBST and incubated with HRP-conjugated anti–rabbit IgG (1:5,000; Cell Signaling) for 1 h at room temperature. Blots were washed for 30 min in TBST and developed with ECL (GE Healthcare).

Live cell imaging

NGF-coated and/or MAG-coated Fluoresbrite YO Carboxylate Microspheres (4.5 or 6.0 μm; Polysciences) were added to cultures of infected DRGs at a low density and allowed to settle for 20 min before imaging. GFP-expressing neurons that contacted a fluorescent protein-bound microparticle were imaged by confocal microscopy using an inverted laser-scanning system (TCS/SP2 LSM; Leica) on an inverted microscope (DMIRE2; Leica) fitted with an environmental chamber to maintain a humidified temperature of 37°C with 5% CO_2. A 63× NA 1.4 oil immersion objective (Leica) was used for all imaging. The pinhole was set for 5 airy U to allow the acquisition of emission over the full thickness of the axon. The 488-nm laser line was used to excite eGFP and fluorescent microparticles; eGFP emission was collected at 498–530 nm, and microparticle fluorescence was collected at 575–600 nm. For time-lapse sequences, images were collected every minute over 50 min using the LCS confocal software package (Leica); the resultant avi file was converted to mov using the QuickTime media player (Apple Computer) and Sorenson compression (Sorenson Media). All image sequences were subjected to identical postprocessing for γ correction.

ImageJ (National Institutes of Health [NIH]) was used to quantify GFP signal intensity in these video sequences using original, unprocessed gray-scale images matched for laser intensity, photo multiplier tube voltage, and offset. For this, pixels/micrometer^2 were quantified in a 10-μm axon segment spanning 5 μm proximally and distally from the center of the particle. The mean signal intensity was determined from five or more axons per condition for at least three separate experiments. Because mRNAs could accumulate before initiation of the imaging sequence, we concentrated our analyses on the t = 50 min images. Unless otherwise indicated, the ratio of mean pixels/micrometer^2 of t = 50 min for NGF- and MAG Fc–treated cultures versus BSA- and IgG Fc–treated cultures, respectively, ± SD is presented. For the db-cAMP–, EHNA-, and siRNA-treated cultures, NGF and MAG signals were compared with similarly treated control cultures (BSA for NGF and IgG Fc for MAG-Fc) for the t = 50 min image.

Effects of siRNAs and EHNA on axonal transport were visualized by live cell imaging of LysoTracker dye (Invitrogen). LysoTracker was added at a final concentration of 50 nM and incubated for 20 min at 37°C. Medium was then changed, and vesicular movement was imaged over 2.5 min, with image acquisition every 5 s. The presence of siGLO signal in the neuronal cell body was used to identify siRNA-transfected neurons. To visualize axonal protein synthesis, infection with the AV-eGFP$^{NLS/myr}$β-actin was concurrent with the siRNA transfection. The NGF- or MAG-coated microparticles were added to cultures, and effects on local synthesis were imaged as described in the beginning of this section.

FISH

FISH was performed as previously described with minor modifications for the DRG cultures (Bassell et al., 1998). Oligonucleotide probes complementary to β-actin mRNA (at positions 3,187–3,138 and 3,446–3,495), peripherin (at positions 868–917, 1,263–1,312, and 1,382–1,431), and Kv3.1a (at positions 3,341–3,390 and 3,045–3,094) were designed using Oligo6 software (Molecular Biology Insights) and checked for homology to other mRNAs by BLAST. Probes were synthesized with amino group modifications at four positions each and labeled with digoxigenin succinamide ester as per manufacturer's instructions (Roche). The DRG cultures were fixed in buffered 4% PFA, equilibrated in 1× SSC with 40% formamide, and incubated at 37°C for 12 h in hybridization buffer (40% formamide, 0.4% BSA, 20 mM ribonucleoside vanadyl complex, 10 mg/ml salmon testes DNA, 10 mg/ml *Escherichia coli* tRNA, and 10 mM sodium phosphate in 1× SSC) containing 20 ng of probe. Hybridization was detected by immunofluorescence using Cy3-conjugated mouse antidigoxigenin (1:1,000; Jackson ImmunoResearch Laboratories); neurofilament protein was detected by colabeling with chicken anti–neurofilament heavy subunit (1:1,000; Chemicon) followed by FITC-conjugated anti–chicken antibody (1:500; Jackson ImmunoResearch Laboratories).

Quantitative imaging of FISH signals was performed on an upright epifluorescent microscope (DM RXA2; Leica) with a CCD camera (ORCA-ER; Hamamatsu). All images were acquired using OpenLab 5.0 software (Improvision) and matched exposure time, gain, and offset with no postprocessing. All quantitative measurements were performed on the original 16-bit images using ImageJ (NIH). The point of the axon corresponding to the center of the particle was used as a reference point for measuring pixel intensity of the Cy3 emission. A 5-μm segment of axon corresponding to 2.5 μm proximal and distal to the particle center was used as the zero point. From this, the pixels/micrometer^2 was quantified in three bins proximal to and distal to the particle center (5-μm length each plus 5-μm bin at particle center). Background was subtracted from the intensity values, and subtracted signal intensity in each 5-μm bin was normalized to the mean intensity over the entire 35-μm axon region that was measured.

Online supplemental material

Table S1 shows array-based identification of axonal mRNAs with the mean intensity of four axonal RNA preparations. Fig. S1 shows the purity of the axonal RNA used to generate the cDNA to probe the arrays (A) and confirms the linear amplification of the cDNA by virtual Northern blotting (B). Fig. S2 shows ^{32}P[UTP] labeling of DRG cultures ± DRB to confirm the effectiveness of RNA polymerase II inhibition (A) and presents a Western blot confirming the reduced levels of dynein heavy chain in DRGs treated with the Dync1h1 siRNA for 72 h (B). Fig. S3 shows cultured DRGs infected with either eGFP$^{NLS/myr}$β-actin 3′ UTR or eGFP$^{NLS/myr}$-γ-actin 3′ UTR reporter constructs. Fig. S4 shows the cultured DRG response to immobilized sources of NGF (A), BSA (B), MAG-Fc (D), or IgG-Fc (E). The figure also shows that pretreatment with K252A before the addition of immobilized NGF shows a requirement for TrkA signaling (C) and that pretreatment with db-cAMP before the addition of immobilized MAG-Fc shows a reversal of MAG's effects by elevation of cAMP signaling (F). Video 1 shows live cell imaging of a neuron exposed to immobilized NGF (video of cell shown in Fig. 5 A). Video 2 shows a neuron pretreated with PD98059 before NGF exposure (video of cell shown in Fig. 5 B). Video 3 shows a DRG pretreated with colchicine before NGF exposure (video of cell shown in Fig. 5 C). Video 4 shows a neuron transfected with Dync1h1 siRNA and stained with LysoTracker to show reduced retrograde but not anterograde transport. Video 5 shows a neuron treated with the dynein inhibitor EHNA and stained with LysoTracker to show reduced retrograde movement. Video 6 shows a neuron exposed to immobilized MAG-Fc (video of cell shown in Fig. 6 A). Video 7 shows a neuron treated with db-cAMP before exposure to immobilized MAG-Fc (video of cell shown in Fig. 6 C). Online supplemental material is available at http://www.jcb.org/cgi/content/full/jcb.200703209/DC1.

Dr. Leslie Krueger (Nemours Biomedical Research) provided technical assistance for design and interpretation of qPCR analyses. The eGFP$^{NLS/myr}$ construct was provided by Dr. Erin Schumann. Dr. Yoshio Goshima provided recombinant Sema3A and the corresponding control protein.

This work was supported by grants from the NIH (NS041696 and NS049041 to J.L. Twiss and HD46368 to G.J. Bassell), the Dr. Miriam and Sheldon G. Adelson Medical Research Foundation, and programmatic funding from the Nemours Foundation. D.E. Willis is supported by a Ruth Kirschstein National Research Service Award (grant NS047821). Centers of Biomedical Research Excellence funds from the National Center for Research Resources/NIH (grant RR020173) provided institutional support for core resources through the Center for Pediatric Research.

Submitted: 31 March 2007
Accepted: 10 August 2007

References

Aakalu, G., W.B. Smith, N. Nguyen, C. Jiang, and E.M. Schuman. 2001. Dynamic visualization of local protein synthesis in hippocampal neurons. *Neuron*. 30:489–502.

Amaldi, F., I. Bozzoni, E. Beccari, and P. Pierandrei-Amaldi. 1989. Expression of ribosomal protein genes and regulatio of ribosome biosynthesis in *Xenopus* development. *Trends Biochem. Sci.* 14:175–178.

Bassell, G.J., and J.L. Twiss. 2006. RNA exodus to Israel: RNA controlling function in the far reaches of the neuron. *EMBO Rep.* 7:31–35.

Bassell, G.J., H. Zhang, A.L. Byrd, A.M. Femino, R.H. Singer, K.L. Taneja, L.M. Lifshitz, I.M. Herman, and K.S. Kosik. 1998. Sorting of beta-actin mRNA and protein to neurites and growth cones in culture. *J. Neurosci.* 18:251–265.

Brumwell, C., C. Antolik, J.H. Carson, and E. Barbarese. 2002. Intracellular trafficking of hnRNP A2 in oligodendrocytes. *Exp. Cell Res.* 279:310–320.

Brunet, I., C. Weinl, M. Piper, A. Trembleau, M. Volovitch, W. Harris, A. Prochiantz, and C. Holt. 2005. The transcription factor Engrailed-2 guides retinal axons. *Nature*. 438:94–98.

Cai, D., Y. Shen, M. De Bellard, S. Tang, and M.T. Filbin. 1999. Prior exposure to neurotrophins blocks inhibition of axonal regeneration by MAG and myelin via a cAMP-dependent mechanism. *Neuron*. 22:89–101.

Cai, D., J. Qui, Z. Cai, M. McAtee, B. Bregman, and M. Filbin. 2001. Neuronal cyclic AMP controls the developmental loss in ability of axons to regenerate. *J. Neurosci.* 21:4731–4739.

Campbell, D.S., and C.E. Holt. 2001. Chemotropic responses of regional growth cones mediated by rapid local protein synthesis and degradation. *Neuron*. 32:1013–1016.

Campbell, D.S., and C.E. Holt. 2003. Apoptotic pathway and MAPKs differentially regulate chemotropic responses of retinal growth cones. *Neuron*. 37:939–952.

Campenot, R.B., and B.L. MacInnis. 2004. Retrograde transport of neurotrophins: fact and function. *J. Neurobiol.* 58:217–229.

Carson, J.H., K. Worboys, K. Ainger, and E. Barbarese. 1997. Translocation of myelin basic protein mRNA in oligodendrocytes requires microtubules and kinesin. *Cell Motil. Cytoskeleton*. 38:318–328.

Chang, L., Y. Shav-Tal, T. Trcek, R.H. Singer, and R.D. Goldman. 2006. Assembling an intermediate filament network by dynamic cotranslation. *J. Cell Biol.* 172:747–758.

Chong, M.S., M.L. Reynolds, N. Irwin, R.E. Coggeshall, P.C. Emson, L.I. Benowitz, and C.J. Woolf. 1994. GAP-43 expression in primary sensory neurons following central axotomy. *J. Neurosci.* 14:4375–4384.

Ekstrom, P., and M. Kanje. 1984. Inhibition of fast axonal transport by erythro-9-[3-(2-hydroxynonyl)]adenine. *J. Neurochem.* 43:1342–1345.

English, A.W., W. Meador, and D.I. Carrasco. 2005. Neurotrophin-4/5 is required for the early growth of regenerating axons in peripheral nerves. *Eur. J. Neurosci.* 21:2624–2634.

Farina, K.L., S. Huttelmaier, K. Musunuru, R. Darnell, and R.H. Singer. 2003. Two ZBP1 KH domains facilitate β-actin mRNA localization, granule formation, and cytoskeletal attachment. *J. Cell Biol.* 160:77–87.

Filbin, M.T. 2003. Myelin-associated inhibitors of axonal regeneration in the adult mammalian CNS. *Nat. Rev. Neurosci.* 4:703–713.

Gu, W., F. Pan, H. Zhang, G. Bassell, and R. Singer. 2002. A predominantly nuclear protein affecting cytoplasmic localization of β-actin mRNA in fibroblasts and neurons. *J. Cell Biol.* 156:41–52.

Hanz, S., E. Perlson, D. Willis, J.Q. Zheng, R. Massarwa, J.J. Huerta, M. Koltzenburg, M. Kohler, J. van-Minnen, J.L. Twiss, and M. Fainzilber. 2003. Axoplasmic importins enable retrograde injury signaling in lesioned nerve. *Neuron*. 40:1095–1104.

He, Y., F. Francis, K.A. Myers, W. Yu, M.M. Black, and P.W. Baas. 2005. Role of cytoplasmic dynein in the axonal transport of microtubules and neurofilaments. *J. Cell Biol.* 168:697–703.

Hill, M.A., L. Schedlich, and P. Gunning. 1994. Serum-induced signal transduction determines the peripheral location of β-actin mRNA within the cell. *J. Cell Biol.* 126:1221–1229.

Huttelmaier, S., D. Zenklusen, M. Lederer, J. Dictenberg, M. Lorenz, X. Meng, G.J. Bassell, J. Condeelis, and R.H. Singer. 2005. Spatial regulation of beta-actin translation by Src-dependent phosphorylation of ZBP1. *Nature*. 438:512–515.

Kaspar, R., D. Morris, and M. White. 1993. Control of ribosomal protein synthesis in eukaryotic cells. *In* Translational Regulation of Gene Expression. Vol. 2. J. Ilan, editor. Plenum Publishing Corp., New York. 335–348.

Kiebler, M.A., and G.J. Bassell. 2006. Neuronal RNA granules: movers and makers. *Neuron*. 51:685–690.

Kislauskis, E.H., X. Zhu, and R.H. Singer. 1994. Sequences responsible for intracellular localization of β-actin messenger RNA also affect cell phenotype. *J. Cell Biol.* 127:441–451.

Lawrence, J.B., and R.H. Singer. 1986. Intracellular localization of messenger RNAs for cytoskeletal proteins. *Cell*. 45:407–415.

Leung, K.M., F.P. van Horck, A.C. Lin, R. Allison, N. Standart, and C.E. Holt. 2006. Asymmetrical beta-actin mRNA translation in growth cones mediates attractive turning to netrin-1. *Nat. Neurosci.* 9:1247–1256.

Li, C., Y. Sasaki, K. Takei, H. Yamamoto, M. Shouji, Y. Sugiyama, T. Kawakami, F. Nakamura, T. Yagi, T. Ohshima, and Y. Goshima. 2004. Correlation between semaphorin3A-induced facilitation of axonal transport and local activation of a translation initiation factor eukaryotic translation initiation factor 4E. *J. Neurosci.* 24:6161–6167.

Lu, P., H. Yang, L.L. Jones, M.T. Filbin, and M.H. Tuszynski. 2004. Combinatorial therapy with neurotrophins and cAMP promotes axonal regeneration beyond sites of spinal cord injury. *J. Neurosci.* 24:6402–6409.

Martin, K.C., and R.S. Zukin. 2006. RNA trafficking and local protein synthesis in dendrites: an overview. *J. Neurosci.* 26:7131–7134.

Ming, G.L., S.T. Wong, J. Henley, X.B. Yuan, H.J. Song, N.C. Spitzer, and M.M. Poo. 2002. Adaptation in the chemotactic guidance of nerve growth cones. *Nature*. 417:411–418.

Nakajima, O., F. Nakamura, N. Yamashita, Y. Tomita, F. Suto, T. Okada, A. Iwamatsu, E. Kondo, H. Fujisawa, K. Takei, and Y. Goshima. 2006. FKBP133: a novel mouse FK506-binding protein homolog alters growth cone morphology. *Biochem. Biophys. Res. Commun.* 346:140–149.

Neumann, S., F. Bradke, M. Tessier-Lavine, and A. Busbaum. 2002. Regeneration of sensory axons within injured spinal cord induced by intraganglionic cAMP elevations. *Neuron*. 34:885–893.

Oleynikov, Y., and R.H. Singer. 2003. Real-time visualization of ZBP1 association with beta-actin mRNA during transcription and localization. *Curr. Biol.* 13:199–207.

Perlson, E., S. Hanz, K. Ben-Yaakov, Y. Segal-Ruder, R. Segar, and M. Fainzilber. 2005. Vimentin-dependent spatial translocation of an activated MAP kinse in injured nerve. *Neuron*. 45:715–726.

Piper, M., and C. Holt. 2004. RNA translation in axons. *Annu. Rev. Cell Dev. Biol.* 20:505–523.

Piper, M., S. Salih, C. Weinl, C.E. Holt, and W.A. Harris. 2005. Endocytosis dependent desensitization and protein synthesis-dependent resensitization in regional growth cone adaptation. *Nat. Neurosci.* 8:179–186.

Piper, M., R. Anderson, A. Dwivedy, C. Weinl, F. van Horck, K.M. Leung, E. Cogill, and C. Holt. 2006. Signaling mechanisms underlying Slit2-induced collapse of *Xenopus* retinal growth cones. *Neuron*. 49:215–228.

Ross, A.F., Y. Oleynikov, E.H. Kislauskis, K.L. Taneja, and R.H. Singer. 1997. Characterization of a beta-actin mRNA zipcode-binding protein. *Mol. Cell. Biol.* 17:2158–2165.

Sasaki, Y., C. Cheng, Y. Uchida, O. Nakajima, T. Ohshima, T. Yagi, M. Taniguchi, T. Nakayama, R. Kishida, Y. Kudo, et al. 2002. Fyn and Cdk5 mediate semaphorin-3A signaling, which is involved in regulation of dendrite orientation in cerebral cortex. *Neuron*. 35:907–920.

Segal, R.A. 2003. Selectivity in neurotrophin signaling: theme and variations. *Annu. Rev. Neurosci.* 26:299–330.

Shan, J., T.P. Munro, E. Barbarese, J.H. Carson, and R. Smith. 2003. A molecular mechanism for mRNA trafficking in neuronal dendrites. *J. Neurosci.* 23:8859–8866.

Shen, Y.J., M.E. DeBellard, J.L. Salzer, J. Roder, and M.T. Filbin. 1998. Myelin-associated glycoprotein in myelin and expressed by Schwann cells inhibits axonal regeneration and branching. *Mol. Cell. Neurosci.* 12:79–91.

Shpetner, H.S., B.M. Paschal, and R.B. Vallee. 1988. Characterization of the microtubule-activated ATPase of brain cytoplasmic dynein (MAP 1C). *J. Cell Biol.* 107:1001–1009.

Smith, D.S., and P. Skene. 1997. A transcription-dependent switch controls competence of adult neurons for distinct modes of axon growth. *J. Neurosci.* 17:646–658.

Snider, W.D. 1994. Functions of the neurotrophins during nervous system development: what the knockouts are teaching us. *Cell*. 77:627–638.

Song, H.J., and M.M. Poo. 1999. Signal transduction underlying growth cone guidance by diffusible factors. *Curr. Opin. Neurobiol.* 9:355–363.

Steward, O., and S. Halpain. 1999. Lamina-specific synaptic activation causes domain-specific alterations in dendritic immunostaining for MAP2 and CAM kinase II. *J. Neurosci.* 19:7834–7845.

Steward, O., C.S. Wallace, G.L. Lyford, and P.F. Worley. 1998. Synaptic activation causes the mRNA for the IEG Arc to localize selectively near activated postsynaptic sites on dendrites. *Neuron*. 21:741–751.

Sundell, C., and R. Singer. 1990. Actin mRNA localizes in the absence of protein synthesis. *J. Cell Biol.* 111:2397–2403.

Tanelian, D.L., M.A. Barry, S.A. Johnston, T. Le, and G.M. Smith. 1997. Semaphorin III can repulse and inhibit adult sensory afferents in vivo. *Nat. Med.* 3:1398–1401.

Tang, S., J. Qiu, E. Nikulina, and M.T. Filbin. 2001. Soluble myelin-associated glycoprotein released from damaged white matter inhibits axonal regeneration. *Mol. Cell. Neurosci.* 18:259–269.

Tapley, P., F. Lamballe, and M. Barbacid. 1992. K252a is a selective inhibitor of the tyrosine protein kinase activity of the *trk* family of oncogenes and neurotrophin receptors. *Oncogene*. 7:371–381.

Tiedge, H. 2005. RNA reigns in neurons. *Neuron*. 48:13–16.

Tongiorgi, E., M. Armellin, P.G. Giulianini, G. Bregola, S. Zucchini, B. Paradiso, O. Steward, A. Cattaneo, and M. Simonato. 2004. Brain-derived neurotrophic factor mRNA and protein are targeted to discrete dendritic laminas by events that trigger epileptogenesis. *J. Neurosci.* 24:6842–6852.

Twiss, J., D. Smith, B. Chang, and E. Shooter. 2000. Translational control of ribosomal protein L4 is required for rapid neurite extension. *Neurobiol. Dis.* 7:416–428.

Verma, P., S. Chierzi, A.M. Codd, D.S. Campbell, R.L. Meyery, C.E. Holt, and J.W. Fawcett. 2005. Axonal protein synthesis and degradation are necessary for efficient growth cone regeneration. *J. Neurosci.* 25:331–342.

Willis, D.E., and J.L. Twiss. 2006. The evolving roles of axonally synthesized proteins in regeneration. *Curr. Opin. Neurobiol.* 16:111–118.

Published September 4, 2007

Willis, D., K.W. Li, J.-Q. Zheng, J.H. Chang, A. Smit, T. Kelly, T.T. Merianda, J. Sylvester, J. van Minnen, and J.L. Twiss. 2005. Differential transport and local translation of cytoskeletal, injury-response, and neurodegeneration protein mRNAs in axons. *J. Neurosci.* 25:778–791.

Wu, D.-Y., J.-Q. Zheng, M.A. McDonald, B. Chang, and J.L. Twiss. 2003. PKC isozymes in the enhanced regrowth of retinal neurites after optic nerve injury. *Invest. Ophthalmol. Vis. Sci.* 44:2783–2790.

Wu, K.Y., U. Hengst, L.J. Cox, E.Z. Macosko, A. Jeromin, E.R. Urquhart, and S.R. Jaffrey. 2005. Local translation of RhoA regulates growth cone collapse. *Nature*. 436:1020–1024.

Yao, J., Y. Sasaki, Z. Wen, G.J. Bassell, and J.Q. Zheng. 2006. An essential role for beta-actin mRNA localization and translation in Ca(2+)-dependent growth cone guidance. *Nat. Neurosci.* 9:1265–1273.

Zhang, H.L., R.H. Singer, and G.J. Bassell. 1999. Neurotrophin regulation of β-actin mRNA and protein localization within growth cones. *J. Cell Biol.* 147:59–70.

Zhang, H.L., T. Eom, Y. Oleynikov, S.M. Shenoy, D.A. Liebelt, J.B. Dictenberg, R.H. Singer, and G.J. Bassell. 2001. Neurotrophin-induced transport of a beta-actin mRNP complex increases beta-actin levels and stimulates growth cone motility. *Neuron*. 31:261–275.

Zheng, J.-Q., T. Kelly, B. Chang, S. Ryazantsev, A. Rajasekaran, K. Martin, and J. Twiss. 2001. A functional role for intra-axonal protein synthesis during axonal regeneration from adult sensory neurons. *J. Neurosci.* 21:9291–9303.

Zweifel, L.S., R. Kuruvilla, and D.D. Ginty. 2005. Functions and mechanisms of retrograde neurotrophin signalling. *Nat. Rev. Neurosci.* 6:615–625.